Quasi-Normal Modes of Scalar Fields in Kerr Background

Master thesis by Vassilis D. Kazazakis

Universiteit van Amsterdam ©

Supervised by Prof. Jan de Boer

Abstract

Quasi-normal modes are all around us. They are the fundamental oscillatory modes of every dissipative system. Excited fields in black hole backgrounds form inherently dissipative systems since energy can be lost either within the black hole or by escaping to infinity. We study the computation of massive scalar field quasi-normal modes in the background of a rotating black hole using the matrix WKB approximation and the monodromy method.

May, 2011 - March, 2012

UNIVERSITEIT VAN AMSTERDAM

FACULTEIT DER NATUURWETENSCHAPPEN, WISKUNDE EN INFORMATICA

INSTITUTE FOR THEORETICAL PHYSICS

Acknowledgements

I am very grateful to my supervisor Prof. Jan de Boer for all the wisdom he shared with me, his sharp comments that would bring me back to earth when I was lost and for all his support. Thank you Jan, it has been an honor working with you.

I am also very grateful to my special friends Teresa and Sasha for all the good times we had talking about physics. Not many people can stand my annoying attitude towards conversations! Thank you for your help, I couldn't have done it without your invaluable friendship.

There are not enough words to express my gratitude towards my family. They have always been there 24/7. Without their unconditional emotional (as well as financial) support, I would not have been able to finish this programme. I love you all!

Thank you Florien! You were there in difficult times.

Special thanks to Stamati Gkaitatzi, Dimitri Palioseliti, Milosz Panfil, Tullio Bagnoli, Rik van Lieshout, Marti Perarnau, Ellen van der Woerd, Olya Shevchuk, Marco Baggio, Ricardo Caldeira, Geoffrey Compere, Marijke Duyvendak, Anne-Marieke Crommentuijn.

Last but not least, my very best friends Antoni and Michali who, though far away, are always there even when they are not! Without them, I would not be the person I am today.

Table of contents

Preface and Overview 9

Conventions 11

1 Introduction 13

1.1 Quasi-normal modes . . . 13

1.1.1 Motivation . . . 13

1.1.2 Definition . . . 14

1.1.3 Physical Significance . . . 16

1.2 Black Holes . . . 17

1.2.1 Schwarzschild black holes . . . 19

1.2.2 Kerr black holes . . . 20

1.3 Klein-Gordon Equation . . . 23

1.3.1 Equations of motion . . . 23

1.3.2 Schwarzschild background . . . 24

1.3.3 Kerr background . . . 25

1.3.4 Teukolsky's Radial Equation . . . 26

2 BTZ QNM: An exactly solvable model 27

2.1 BTZ metric . . . 27

2.2 The equation . . . 27

2.3 Solution . . . 28

2.3.1 The hypergeometric equation . . . 29

2.4 Boundary conditions . . . 30

2.4.1 Condition at the horizon . . . 30

2.4.2 Condition at infinity . . . 30

3 WKB Approximation **33**

3.1 WKB Approximation . . . 33

3.2 Matrix WKB method . . . 34

3.3 Properties of the **F** matrix . . . 37

3.4 Estimates for the connection matrix **F**, $\mathbb{R}$eal $Q^2(x)$ . . . 38

3.4.1 General considerations . . . 38

3.4.2 Two points in the same classically *allowed* region . . . 39

3.4.3 Two points on opposite sides of a classical turning point . . . 39

3.4.4 Two points on opposite sides of a potential barrier . . . 41

3.5 Estimates for the connection matrix **F**, $\mathbb{C}$omplex $Q^2(z)$ . . . 42

3.5.1 Stokes' and anti-Stokes' lines . . . 43

3.5.2 Region around a first order zero of $Q^2(z)$ . . . 43

3.5.3 Stokes' phenomenon . . . 44

3.6 Quasi-normal modes and the WKB approximation . . . 44

3.6.1 Ansatz . . . 45

3.6.2 Boundary conditions . . . 45

3.6.3 One turning point . . . 46

3.6.4 Two turning points . . . 46

3.6.5 Three turning points . . . 47

4 Monodromy Method **49**

4.1 Monodromy Technique . . . 49

4.2 Monodromy: an example . . . 50

4.3 Quasi-normal modes and the monodromy method . . . 51

4.3.1 Monodromy Φ_1 . . . 52

4.3.2 Monodromy Φ_2 . . . 53

4.3.3 The QNM generating equation . . . 56

5 QNM Numerics & Computation **57**

5.1 Numerical Solutions . . . 57

5.2 Matrix WKB . . . 57

5.2.1 Computing the error τ . . . 58

5.2.2 Computing the roots of Q^2 . . . 58

5.3 Monodromy . . . 59

6 Conclusions **63**

6.1 Matrix WKB approximation 63

6.2 Monodromy method 64

6.3 Outlook 65

Appendices **69**

A Spheroidal Functions **69**

A.1 Spheroidal coordinates 69

A.2 Spheroidal differential equations 70

A.3 Power series expansion for λ_{mn} 71

A.4 Asymptotic expansions of λ_{mn} 71

B The Hypergeometric Function **73**

B.1 The hypergeometric differential equation 73

B.2 The solution 73

C Mathematica Source Code **75**

C.1 Monodromy source code 75

Preface and Overview

This master thesis was done as part of the "*Theoretical Physics*" master programme of the University of Amsterdam during the period 04/2011 - 12/2011 under the supervision of Professor Jan de Boer. Its goal has been to study two specific methods for the calculation of quasi-normal modes of massive scalar field in the background of a rotating black hole.

Chapter 1 serves to introduce the reader into the topic by explaining what quasi-normal modes are and why we are interested in them. Some basic background material is given into black hole spacetimes, first to the simplest case of Schwarzschild black hole and next to its rotating version, Kerr. Last, the scalar field equation is introduced and separation of variables is performed.

Chapter 2 is aimed to be self-contained. We study the scalar quasi-normal modes of the BTZ black hole (2+1 dimensions). This work was carried out as an introduction to the subject. It serves this purpose well since it is a simple and exactly solvable model, not only for its quasi-normal frequencies but also for the scalar field density.

In Chapter 3 we study the first method for deriving the quasi-normal modes, the matrix WKB approximation. Having found that most papers on the subject do not give the appropriate background for the use of this method, we took this opportunity to give a much more detailed analysis. However, it would be impossible to be completely thorough and the reader is referred to the literature for more details. Lastly, we apply the method and derive the quasi-normal mode generating equations.

In Chapter 4 we study the second method for solving our problem, the monodromy method. After explaining what the method is about, we apply it on the scalar field equation and derive an analytic formula for the quasi-normal frequencies.

Chapter 5 is devoted in getting actual values for the quasi-normal frequencies through numerical means. After concluding that the matrix WKB does not work through our approach to the problem, we successfully calculate the quasi-normal frequencies by using the formula from the monodromy method.

Notation, definitions, conventions and useful relations

A problem that often arises when one does research in physics is the many conventions that are in use at the same time. Different authors, even in the same topic, use different symbols and units to describe and talk about the same concept.

One of the first difficulties that we encountered in the writing of this thesis was that such conventions were not always explicit and in some cases even completely unclear. In order to not put the reader through the same ordeal, the conventions used in this work will be presented before anything else. What is more, we will take advantage of this opportunity to present some useful definitions and formulas that will be used later on.

Planck's units, also known as *natural units*, are best suited for the work that follows it being mainly theoretical.

- Gravitational constant $G = 1$
- Speed of light $c = 1$
- Reduced Planck's constant $\hbar = 1$
- Coulomb's constant $k_e = \dfrac{1}{4\pi\epsilon_0} = 1$
- Boltzmann's constant $k_{\mathrm{B}} = 1$

The equivalent of 1 Planck unit in SI

Length	$1.616 \cdot 10^{-35}\,\mathrm{m}$
Mass	$2.177 \cdot 10^{-8}\,\mathrm{kg}$
Frequency	$1.855 \cdot 10^{43}\,\mathrm{Hz}$
Temperature	$1.417 \cdot 10^{32}\,\mathrm{K}$

ω	(quasi-normal) frequency.
n	harmonic number.
$r_\pm$	horizons of the Kerr black hole. r_+ is the event horizon while r_- is a Cauchy horizon.
M	ADM mass.
J	angular momentum in natural units.
a	normalized angular momentum (angular momentum per unit mass). The term "normalized" is often omitted. For a Kerr black hole, $a < M$.
l, m	magnetic & azimuthal quantum numbers.
κ, ρ, ν, σ	indices labeling components of covariant quantities.
$g_{\kappa\nu}$ $(g^{\kappa\nu})$	spacetime's metric tensor (and its inverse).
g	metric's determinant $g = \det g_{\kappa\lambda}$.
μ	scalar field's mass.
$M_\odot$	Solar mass
Λ	Cosmological constant

- Metric sign convention $\eta_{\mu\nu} = \mathrm{diag}(-1, 1, 1, 1)$
- For $z = x + iy \in \mathbb{C}$, $\Re(z) = x$ and $\Im(z) = y$
- $\dfrac{\partial \det(\mathbf{A})}{\partial a} = \det(\mathbf{A}) \mathrm{tr}\left(\mathbf{A}^{-1} \dfrac{\partial \mathbf{A}}{\partial a}\right)$

$$\mathbf{M} = \begin{pmatrix} M_{11} & M_{12} & \cdots & M_{1n} \\ M_{21} & \ddots & & \vdots \\ \vdots & & \ddots & \vdots \\ M_{n1} & M_{n2} & \cdots & M_{nn} \end{pmatrix}$$

ADM Charge	Charge (energy, angular momentum, etc) as measured from infinity
BH	Black Hole
BTZ	Black hole solution in 2+1 dimensions named after Banados, Teitelboim and Zanelli
CFT	Conformal Field theory
GR	General Relativity
KG	Klein-Gordon
QFT	Quantum Field theory
QM	Quantum Mechanics
QNM	Quasi-normal mode(s)

CHAPTER 1

Introduction

1.1 Quasi-normal modes

1.1.1 Motivation

It is known that most objects around us, like a bell or a drum, produce very specific sounds when excited appropriately (e.g. "hit"). These sounds are characteristic to each object which respond to such excitations with a superposition of different oscillatory modes. Take, for example, a guitar string. No matter how you pull it, the sound it produces will always be recognizable as a specific note.

Black holes are not much different in that respect. They also have a set of natural frequencies. However, what is now oscillating are fields in the BH vicinity or even spacetime itself rather than pressure in a gas producing sound waves. As such, these frequencies characterize the behavior of fields in the region immediate to a BH. This has been verified both by fully numerical simulations of BH systems as well as theoretically at a perturbative linearized level. As a result, they are a characteristic of BH.

These oscillations are called "*quasi-normal modes*" and the frequencies associated to them "*quasi-normal frequencies*". Their name is inspired from ordinary normal modes & frequencies from which, however, they do differ substantially.

A system that oscillates in a purely normal mode, is never going to stop, i.e. normal modes are stationary states. Many basic systems can be adequately modeled by such a scheme. The modelling of a pendulum, for example, can usually be quite accurate without taking into account that friction will eventually stop it. However, this is not always the case. Quasi-normal modes are exponentially damped due to the system's energy loss. No matter the mechanism, which in the case of BH is emittion of radiation (gravitational or other), they offer a much more realistic and precise picture of reality.

The second difference between them is quite more theoretical. The exponential damping of a mode suggests that it can appear for only a finite (limited) amount of time. In mathematical

terms, this means that they do not form a complete set in terms of being able to express *any* signal as a superposition of quasi-normal modes. This is in contrast to normal modes whose completeness is a valuable tool in Physics and Mathematics in general. This tool is also known as "Fourier transform".

More detailed information on the subject, along with this work, can be found in the excellent works [1; 2] and references therein.

1.1.2 Definition

Quasi-normal modes model the late time behavior of perturbed compact objects. In our case, it is the BH spacetime as well as fields in its vicinity that are excited and which we study at a linearized level. This thesis concentrates on scalar field perturbations. What is said in this section, though, is generally applicable to other fields as well.

In most, if not all cases, the study of the field in question can be reduced to a second order differential equation of the form

$$\frac{d^2\phi_s}{dx^2} + Q_s^2\left(\omega,\, x\right)\phi_s = 0 \tag{1.1.1}$$

where x is related to a spatial variable (usually radial distance from the center of the BH), ω is the (quasi-normal) frequency and s is the spin of the field under study[1]. Time dependence is assumed to be of the form $\exp\left(-i\omega t\right)$ which, though seemingly restrictive, it is not due to time translational invariance.

Q_s^2 will be referred to as the generalized potential, due to its relation to the Schrödinger equation (where, usually, $Q^2 = E - V$). Its form, as well as the relation between ϕ_s and the actual field density are dependent on the specifics of the BH spacetime as well as the type of the field itself (scalar, spinor, vector, etc). In special cases, such as Schwarzschild BH, it takes the simpler form $Q_s^2 = \omega^2 - V_s(x)$, see §1.3.2. Variable x has similar dependencies and *usually* ranges in all $\mathbb{R}$ with $-\infty$ being the BH's event horizon and $+\infty$ the actual spatial infinity.

The physical problem studied requires that there are no other sources of waves. The settling down of the excitation we are studying is the only source. Mathematically, this means that at spatial infinity, only outgoing wave solutions should be allowed, i.e.

$$\phi_s \sim \exp\left(+i\Omega_+ x\right), \quad \text{for} \quad x \to +\infty \quad \text{and} \quad Q_s(+\infty) = \Omega_+ \tag{1.1.2}$$

A similar argument applies on the other boundary of our problem, at $x \to -\infty$. The very nature of a BH's event horizon along with preservation of causality disallows any outgoing solutions. By definition, matter and energy (which includes any field, either massive or massless) can only go further into the BH once they cross it. Similar to before, mathematically, this means that at the horizon only ingoing wave solutions should be allowed, i.e.

$$\phi_s \sim \exp\left(-i\Omega_- x\right), \quad \text{for} \quad x \to -\infty \quad \text{and} \quad Q_s(-\infty) = \Omega_- \tag{1.1.3}$$

[1] $s = 0$ for a scalar, $s = \pm 1$ vector, $s = \pm 2$ tensor and $s = \pm {}^1/_2$ spinor

The frequencies $\Omega_\pm$ depend on the frequencies ω and potentially on the rest of the problem's parameters. It is only a discrete set of complex frequencies ω that give solutions satisfying the aforementioned boundary conditions. These are the ones called *quasi-normal frequencies*. From the field's time dependence $\exp(-i\omega t)$, it is easy to see that it is the imaginary part of ω that models the damping (exponential decay) and thus the dissipative effect. What is more, it is evident that $\Im\omega$ must be strictly *not positive*[2] since in the opposite case, the field will diverge for large times (which is of course unphysical).

An example: Damped vibrating string

A fairly familiar and related model is the following. Consider a champagne glass which is "excited" (e.g. hit carefully with a knife!). The frequencies of the soundwaves produced by it are quantized. Whatismore, the system's inherent dissipativeness due to the escape of energy through soundwaves, makes those frequencies complex. Their imaginary part corresponds to the characteristic timescale of each mode.

A simple model for this phenomenon is that of a vibrating string with a velocity-dependent force term (friction) and periodic boundary conditions. The wave equation in such a case is

$$T\frac{\partial^2 u}{\partial x^2} - k\frac{\partial u}{\partial t} - \rho\frac{\partial^2 u}{\partial t^2} = 0 \tag{1.1.4}$$

Here, T is the string's tension, k encodes the strength of the dissipative effects [3] and ρ is the mass density. We impose the ansatz $u(x,t) = \exp(-i\omega t)\,X(x)$ and the equation above reduces to

$$X'' + \Omega^2 X = 0 \quad \text{where} \quad \Omega^2 = \frac{\rho\omega^2 + ik\omega}{T} \tag{1.1.5}$$

This is the equation of a simple harmonic oscillator. Its solution is easily obtained in terms of complex exponentials and is given by $X_\pm(x) = \exp(\pm i\Omega x)$. However, we still have to apply boundary conditions. Our model implies that we have to impose that the system "closes", i.e. periodic boundary conditions, so that $X_\pm(0) = X_\pm(L)$, where L is the length of the string (or by analogy, the circumference of the glass). This condition gives us the *quasi-normal frequency* generating equation

$$\exp(\pm i\Omega L) = 1 \quad \Rightarrow \quad \Omega = \frac{2\pi}{L}n\,, \quad n \in \mathbb{N} \tag{1.1.6}$$

Solving with respect to ω with the help of (1.1.5) we get that

$$\boxed{\omega_n = \pm\frac{\sqrt{16\pi^2 T\rho\, n^2 - k^2 L^2}}{2L\rho} - i\frac{k}{2\rho}\,, \quad n \in \mathbb{N}} \tag{1.1.7}$$

These frequencies are termed quasi-normal frequencies of the system. Note that should there be any frequencies with $\Im(\omega_n) > 0$ their whole system would be discarded as it represents an unphysical solution for $t \to \infty$ (the solutions blow up).

[2] i.e. zero or negative

[3] only includes effects which can be modelled as velocity-proportional forces

1.1.3 Physical Significance

The study of quasi-normal modes of black holes is very important in physics. Black holes are *the* extraordinary object of GR. They can be suppermassive BH residing in galactic centers or solar sized ones, remnants of dead stars. Despite the enormous complexities of such objects, BH can be modelled completely with only a few parameters. They are considered the very basic objects of GR, much like the hydrogen atom is in quantum mechanics.

As such, there is much to learn by studying their interactions with fields around them. What is more, being usually very massive, they make an excellent candidate for testing the theory of GR in the strong field regime, something that has not been done yet in an adequate way.

BH parameter estimation

Historically, the first BH related QNM to be studied where those of gravitational waves. The study of the binary pulsar PSR B1913+16 [3] was the first experimental indication to their existence. The observed increase in the pulsar's frequency could very well be explained by the spiralling-in of the binary due to energy loss from radiating gravitational waves. Gravitational wave astronomy is now a new field of astrophysics aiming (amongst others) to the direct detection and measurement of gravitational waves.

Gravity being so weak, compared to the rest of the fundamental forces, makes the detection of gravitational waves an extremely delicate process. With current detector technology, it is only but the most violent gravitational phenomena that we expect to see, such as black hole collisions, stellar collapses, etc. Theoretical considerations along with numerical simulations indicate that the late time behavior of such processes (even though they are not stationary) can very well be approximated by a superposition of QNM. As a result, since QNM depend on BH parameters only, detecting gravitational waves and fitting them to QNM models will, in principle, allow us to measure these parameters. More on the specifics of such computations can be found in [4] and references therein.

However, in this thesis, we only study scalar perturbations, i.e. $s = 0$, and the resulting QNM are not directly applicable to gravitational waves ($s = 2$). Nevertheless, the form of Q_s^2 in both cases is not much different (see §1.3.4) and the techniques presented in this thesis are still in principle applicable.

Gauge-gravity duality

Another important field of interest for the application of QNM is string theory and the AdS/CFT correspondence, also known as the Maldacena duality. The correspondence is the conjectured equivalence between string theory and gravity on a spacetime of N dimensions with negative cosmological constant Λ and a conformal quantum field theory defined on an $(N-1)$-dimensional space without gravity. It has been useful for the calculation of many quantities of strongly coupled systems which would have otherwise been next to impossible.

According to the duality, a black hole in AdS spacetime corresponds to an approximately thermal state of a strongly coupled system in the CFT. As a result, knowledge of the BH's QNM allows us to model the behavior of the thermal state, something that would otherwise be much more difficult owning to its strongly coupled nature. More specifically, QNM coincide with the poles of correlation functions. Effectively, they correspond to quasi-particles in the CFT side.

The spacetime we are studying in this thesis is asymptotically Minkowski, i.e. $\Lambda = 0$ (except from Ch.2), and thus our results do not directly apply. However, there are generic features of the dependence of the modes on the parameters which remain true for AdS. What is more, the computations do not differ substantially and the techniques presented are still applicable. For more details, the reader is referred to [1] and references therein.

BH area quantization

String theory is not the only candidate for a theory of quantum gravity. Attempts are still made for the study of BH in the context of QFT. Bekenstein conjectured [5] that the area of a BH's event horizon takes on a discreet value spectrum resulting in the quantization of the BH's mass as well.

Semi-classical arguments suggest that $\Delta M = \Delta\omega$ in the highly damped limit. What is more, within loop quantum gravity, an alternative approach to a theory of quantum gravity, knowledge of the QNM spectrum may allow one to fix an otherwise unknown parameter (known as Barbero-Immirzi parameter) which shows up in the formula for the area of a BH.

All these point to a potentially fundamental relation between QNM and a theory of quantum gravity. However, such suggestions are still highly theoretical and more research is required. Study of BH spectrum will help advance such research. More can be found in the literature.

1.2 Black Holes

> "*A black hole is a region of space from which nothing, not even light, can (classically) escape.*"

Black holes are the fate of all massive stars. They form when there is no mechanism left for a star to resist gravitational collapse. In less massive cases, such mechanisms are electron and neutron degeneracy pressure for brown dwarfs and neutron stars respectively.

Viewed from the outside, what sets the black hole apart from other black objects is that there is a minimum distance one can approach after which there is no turning back – point of no-return. A black hole's mass is concentrated on one single point (or a one-dimensional ring in the case of a rotating BH) of infinite density. Its boundary is considered to be an invisible and immaterial surface, called the "*event horizon*", which marks the point of no return.

A feature that makes black holes so attractive to physicists (besides their mass!) is their extraordinary simplicity. Even though they are formed by objects of practically almost infinite degrees of freedom, we only need a limited number of parameters to completely describe them. To fully appreciated this, think of the following: a complete classical description of, say, a planet, would require precise knowledge of the position and velocity of every particle from which it is made of. For Earth, this translates to $\mathrm{O}\left(10^{51}\right)$ degrees of freedom in contrast to a black hole which, as we shall see later on, has $\mathrm{O}\left(10^{1}\right)$.

For stationary black holes solutions of the Einstein-Maxwell theory of gravitation and electromagnetism this postulate takes the form of the "*no-hair theorem*"[5; 6]. The theorem states that a stationary black hole can be completely described by only three parameters: mass, electric charge [4] and angular momentum (along, of course, with its position, velocity and orientation). Other physical properties of matter such as the *baryonic, leptonic* and other conserved numbers seem to be irretrievably lost once the black hole is formed.

All this seems to denote that physical information could disappear within the black hole contrary to quantum physics. Unitary evolution, as dictated by QM, is time symmetric and hence a reversible process. As a result, a quantum state cannot be destroyed and information must be conserved. However, the small number of parameters that are needed to describe a black hole show that many different quantum states can evolve into one and only. Consequently, the phase space of each set of BH parameters is enormous suggesting that the initial state and information are essentially lost or even destroyed.

It has been shown [7] that a black hole is not really that black after all. It emits radiation which is exactly thermal. This opens the issue of the *black hole information paradox*[8]. By emitting thermal radiation[5], a black hole will eventually evaporate essentially destroying all information that has fallen into it. Various methods and solutions have been proposed (see e.g. [9; 10]) but, to date, none is generally accepted.

In the Einstein-Maxwell theory, there exist different families of black hole solutions characterized by which parameters are zero. These solutions also differ according to the value of the cosmological constant Λ (positive, negative or zero). Current data [11; 12] indicate that it is small but nonzero and positive. Various equations can be simplified in the absence of this constant. In this thesis, we are going to take advantage of that by studying the case of $\Lambda = 0$. This can be justified by its "small" value which, in many cases, shall make this study relevant even if $\Lambda \neq 0$.

According to the aforementioned, the different black hole solutions are summarized on the following table:

$\Lambda = 0$	Non-rotating ($J = 0$)	Rotating ($J \neq 0$)
Uncharged ($Q = 0$)	Schwarzschild	Kerr
Charged ($Q \neq 0$)	Reissner-Nordström	Kerr-Newman

[4] The theory also allows a magnetic charge. Since however no magnetic monopoles have been detected to date, we shall not consider this case

[5] By definition, thermal radiation cannot carry any information

For astrophysical black holes, we expect that $Q \sim 0$ since any non-negligible deviation will attract opposite charge particles and bring the black hole back to an electrically neutral state. As a result, we shall not consider the $Q \neq 0$ case at all.

1.2.1 Schwarzschild black holes

The simplest black hole solution one can look into is the non-rotating uncharged case. Starting from Einstein's equations, the imposition of spherical symmetry yields a unique solution in vacuum. [6] This uniqueness was first proven by Jebsen and later by Birkhoff[13] after whom it was named as "*Birkhoff's Theorem*" (see [14] for a detailed proof).

For asymptotically flat spacetimes, i.e. $\Lambda = 0$, this unique solution is given by the Schwarzschild metric which, in spherical coordinates, is given by [14; 15]

$$\boxed{ds^2 = -\left(1 - \frac{2M}{r}\right) dt^2 + \frac{dr^2}{\left(1 - \frac{2M}{r}\right)} + r^2 \left(d\theta^2 + \sin^2\theta d\phi^2\right)} \tag{1.2.1}$$

The constant M can be identified with the gravitational mass of the body as measured from spatial infinity (ADM mass).

This solution is valid outside of any massive object with spherical symmetry. Trivial inspection of (1.2.1) shows that there are apparent singularities at $r = 2M$ (also known as *Schwarzschild* or *gravitational* radius r_g) and $r = 0$. However, these could be just coordinate singularities so care must be taken in examining them.

Event horizon, $r = 2M$

By transforming to **Kruskal-Szekeres** coordinates T, R given by

$$T = \exp\left(\frac{r}{4M}\right) \sinh\left(\frac{t}{4M}\right) \sqrt{\pm\left(\frac{r}{2M} - 1\right)} \tag{1.2.2a}$$

$$R = \exp\left(\frac{r}{4M}\right) \cosh\left(\frac{t}{4M}\right) \sqrt{\pm\left(\frac{r}{2M} - 1\right)} \tag{1.2.2b}$$

where the $+(-)$ sign applies outside(inside) the horizon, the metric becomes

$$ds^2 = \pm\frac{32M^3}{r} e^{-r/2M} \left(-dT^2 + dR^2\right) + r^2 d\Omega_2^2 \tag{1.2.3}$$

with r now being an implicit function of T and R given by

$$T^2 - R^2 = \pm\left(\frac{r}{2M} - 1\right) e^{r/2M} \tag{1.2.4}$$

The event horizon at $r = 2M$ is given by $R = \pm T$ in the new coordinates and it is evident that it was just a coordinate singularity now being completely well behaved.

[6] In this context, by vacuum solution it is meant that the metric is only valid *outside* a spherical body in absence of any other matter/energy.

Interesting physics do take place there though. Study of the lightcone structure of the metric reveals that for $r < 2M$, the lightcones point entirely to smaller radii. This means that anything that crosses the boundary at $r = 2M$ will undoubtedly proceed to smaller radii until it reaches $r = 0$. As a result, the gravitational radius marks the boundary and point of no return of the Schwarzschild BH.

However, direct numerical computation shows that almost always, these radii are extremely small. This BH solution being applicable only in vacuum, the gravitational radius is relevant *only* if it lies outside the gravitating body. As a result, for most objects such considerations do not apply. For example, for the sun $r_g \sim 3$km while for the Earth, $r_g \sim 9$mm. In such cases, one has to "glue" this solution with one appropriate for the inside of the object.

True singularity, $r = 0$

Let us take a better look at the other singular point of the Schwarzschild metric, $r = 0$. Note in (1.2.3) that even though we managed to get rid of the apparent singularity at $r = 2M$, $r = 0$ still remains singular. In fact, it is impossible to find a coordinate system which is not singular there. This can be seen by taking a different approach. Scalar quantities in GR are independent of the coordinate system used. Direct computation shows that

$$R^{\kappa\nu\rho\sigma} R_{\kappa\nu\rho\sigma} = \frac{48M^2}{r^6} \tag{1.2.5}$$

where $R^{\kappa}{}_{\nu\rho\sigma}$ is the Riemann tensor. It is now evident that $r = 0$ is a true curvature singularity of the Schwarzschild spacetime.

The big picture

The picture is now clear. When a spherically symmetric mass becomes so small (e.g. by gravitational collapse) that its radius becomes less than its Schwarzschild radius an event horizon is formed. Once that happens, the object continues to contract until all mass is concentrated at $r = 0$, a point where mass density, curvature and tidal forces in its vicinity are infinite. Anything that approaches close enough to cross the spherical surface at $r = 2M$ will inevitably continue towards the singularity which it will reach in finite proper time.

1.2.2 Kerr black holes

The Schwarzschild black hole provides the perfect pedagogical tool for an introduction to general relativity and black holes. However, it remains a poor model for astrophysical and experimental purposes.

Most, if not all, astrophysical black holes are created by either dying stars or large accretions of matter (galactic nuclei) where, in both cases, the masses involved have angular momentum (which of course must be conserved). This makes the Schwarzschild solution inapplicable since spherical symmetry is broken. Instead, there is only axial symmetry now.

With a calculation similar to the Schwarzschild case, Kerr, in 1963 while trying to find the solution for an axially symmetric, rotating object came up with a solution which in **Boyer-Lindquist** coordinates is expressed as [14; 15]:

$$\begin{aligned} ds^2 = &+ \frac{\rho^2}{\Delta} dr^2 + \rho^2 d\theta^2 + \left[\left(r^2 + a^2\right) \sin^2\theta + \frac{2Mr}{\rho^2} a^2 \sin^4\theta \right] d\phi^2 - \\ &- \frac{4Mr}{\rho^2} a \sin^2 d\phi dt - \left(1 - \frac{2Mr}{\rho^2}\right) dt^2 \end{aligned} \tag{1.2.6}$$

$$\Delta = r^2 - 2Mr + a^2, \qquad \rho^2 = r^2 + a^2\cos^2\theta, \qquad g \equiv det(g_{\mu\nu}) = -\rho^4 \sin^2\theta \tag{1.2.7}$$

It will be useful to have the contravariant metric $g^{\mu\nu}$ as well which we quote here

$$\begin{aligned} \left(\frac{\partial}{\partial s}\right)^2 = \frac{1}{\rho^2} \Bigg\{ &\Delta \left(\frac{\partial}{\partial r}\right)^2 + \left(\frac{\partial}{\partial \theta}\right)^2 + \left(\frac{1}{\sin^2\theta} - \frac{a^2}{\Delta}\right) \left(\frac{\partial}{\partial \phi}\right)^2 - \\ &- \frac{4Mra}{\Delta} \frac{\partial}{\partial \phi} \frac{\partial}{\partial t} - \left[\frac{\left(r^2 + a^2\right)^2}{\Delta} - a^2 \sin^2\theta \right] \left(\frac{\partial}{\partial t}\right)^2 \Bigg\} \end{aligned} \tag{1.2.8}$$

Here, M is the black hole's ADM mass while a is related to its ADM angular momentum J via $J = aM$. Moreover, the r, θ, ϕ coordinates are not the usual spherical coordinates (though they do reduce to them for $a = 0$) but rather the *oblate spherical coordinates* (see App. A.1). Notice that the metric describing a black hole rotating the "other way", i.e. $a \to -a$, remains invariant if we also transform $\phi \to -\phi$. This is to be expected since right-handed rotation should be no different than left-handed. As a result, with no loss of generality, we can take a to be positive.

It has to be noted that there have not be found any interior solutions with physical matter that fit smoothly to a Kerr exterior. This means that the Kerr solution cannot be used for material body, contrary to the Schwarzschild solution. However, the limit $a \to 0$ correctly reproduces the Schwarzschild solution (as expected).

As before, there should be interesting physics taking place around points where the metric is singular, namely $\rho^2 = 0$, $\Delta = 0$ and $\left(1 - {}^{2Mr}/_{\rho^2}\right) = 0$. Let us investigate those one by one.

Singularity, $\rho^2 = 0$

As in the Schwarzschild case, by calculating the appropriate scalar, one can show that $\rho^2 = 0$ indeed corresponds to a true curvature singularity rather than a coordinate one. It occurs where $r^2 + a^2\cos^2\theta = 0$ which can only be satisfied if $r = 0$ *and* $\theta = \pi/2$ at the same time. Even though this might seem strange it is not. Remember that r and θ are not the standard spherical coordinates. Let us transform to the more convenient Cartesian coordinates via (see App. A.1):

$$x = \sqrt{r^2 + a^2} \sin\theta \cos\phi \,, \quad y = \sqrt{r^2 + a^2} \sin\theta \sin\phi \,, \quad z = r\cos\theta \tag{1.2.9}$$

In the (x, y, z) coordinate system, surfaces of constant r are confocal ellipsoids whose principal axis coincide with the coordinate axis. It is now evident that $r = 0$ is not a point but corresponds to the disk $x^2 + y^2 = a^2 \sin^2\theta,\ z = 0$ so that singularity occurs at the ring

$$x = a\cos\phi, \quad y = a\sin\phi, \quad z = 0 \tag{1.2.10}$$

Horizons, $\Delta = 0$

Using the appropriate coordinate transformation (see [16] and references therein) one can show that the singularities of $\Delta = 0$ are merely coordinate ones. They correspond to a Cauchy horizon ($r = r_-$) and an event horizon ($r = r_+$) given by

$$r_\pm = M \pm \sqrt{M^2 - a^2}\,, \quad r_- < r_+ \tag{1.2.11}$$

Note that for $a = 0$, the Schwarzschild limit, the outer horizon coincides with the Schwarzschild event horizon $r_+ = r_g$. We thus identify r_+ with the event horizon of the Kerr black hole.

It is important to note that Δ has no real zeros if $a > M$. In such a case, we see that there is no horizon to cover the singularity and the solution is thus called a "*naked singularity*". It can be shown that such spacetimes possess various undesirable properties (like closed time-like curves) and are thus considered unphysical.

Penrose, 1969, formulated the *cosmic censorship conjecture*. It asserts that spacetime singularities forming from graviational collapse of matter should always be hidden behind event horizons. Moreover, it suggests that on order for a Kerr BH to be physical $a \leq M$ must hold. However, it can be shown [17; 18] that a Kerr black hole with $a < M$ can never acquire enough angular momentum so that $a = M$ and thus can never evolve into a naked singularity. As a result, in this thesis, we will only be concerned about the case $a < M$.

The ergosphere

The ergosphere is a hypersurface given by

$$r = M + \sqrt{M^2 - a^2\cos^2\theta} \geq r_+ \tag{1.2.12}$$

This "radius" (notice the θ dependence) marks the surface where the frame-dragging due to the rotation of the black hole drags spacetime into corotation with a tangential velocity equal to that of light. No observer can remain angularly stationary with respect to infinity since that would require them to exceed the speed of light.

This has notable effects since energy can be extracted from the black hole through the Penrose process which goes as follows. A lump of matter enters the ergosphere while staying out of the event horizon. Once there, it splits into two pieces whose four-momentum can be appropriately arranged so that one piece escapes to infinity while the other falls into the black hole. It is possible for the piece that escapes to infinity to have a greater energy than the original one.

The extra energy has been extracted from the rotational energy of the black hole. This is achieved since, with respect to infinity, the infalling piece has negative energy (though with respect to its local frame it is of course positive) and thereby by conservation of energy the outgoing piece has more energy than it did originally.

1.3 Klein-Gordon Equation

In theoretical physics, a field which is invariant under Lorentz transformations is called a "scalar" in contrast to a spinor or vector/tensor field. This difference translates to, among others, a difference in spin of the field quanta, i.e. particles.

Scalar particles have zero spin, vector/tensor particles integer spin while fermions, i.e. particles of a spinor field, half-integer. In nature, all fundamental fields that have been observed so far are known to have non-zero spin. The hypothetical Higgs boson, if observed, will be the first example of spin zero fundamental particle.

In light of the aforementioned, it might be difficult for one to see the merits of studying scalar fields. However, many physical phenomena have effective field theories in which scalar fields play a central role. A set of examples is the case of the pi mesons $(\pi^0, \pi^\pm)$ which, while composite particles, in low energies can be treated as scalar fields.

Moreover, scalar fields are mathematically simpler to study than others and can often provide good insight into complex problems. This thesis presents a good example. From an astrophysical point of view, we are interested in quasi-normal modes of the graviton which is a spin-2 particle. Mathematical study of such waves includes vector modes (spin-1) as well as scalar modes (spin-0). As a result, studying the scalar case also addresses part of a bigger problem. More details on this shall be presented shortly in §1.3.4.

1.3.1 Equations of motion

Scalar fields are described by the *Klein-Gordon* equation (sometimes referred to as the Klein-Fock-Gordon equation). It was introduced by physicists Oskar Klein and Walter Gordon in 1927 as a proposed description for relativistic electrons. Though wrong for that matter (the Dirac equation is the correct equation for electrons), its theoretical value was soon appreciated.

The Lagrangian for the Klein-Gordon field in curved spacetime with the $(-,+,+,+)$ metric convention is [14]:

$$\mathcal{L} = -g^{\kappa\nu}\nabla_\kappa\phi\nabla_\nu\phi^* - \mu^2\phi^*\phi \tag{1.3.1}$$

$g^{\kappa\nu}$ is the (inverse) metric tensor describing the spacetime in which the field propagates and μ is the field particle's mass. ∇_κ is the covariant derivative which in this case coincides with a partial derivative since it acts on a scalar. In the case of a vector it would be $\nabla_\kappa V^\nu = \partial_\kappa V^\nu + \Gamma^\nu_{\kappa\rho}V^\rho$ where $\Gamma^\nu_{\kappa\rho}$ is the Christoffel connection of the metric space at hand.

Using the Euler-Lagrange equations for ϕ^*

$$\nabla_\kappa \left(\frac{\partial \mathcal{L}}{\partial \left(\nabla_\kappa \phi^* \right)} \right) - \frac{\partial \mathcal{L}}{\partial \phi^*} = 0 \tag{1.3.2}$$

we get the massive scalar field equation

$$\left(\Box - \mu^2 \right) \Phi = 0 \tag{1.3.3}$$

where $\Box = \nabla_\nu \nabla^\nu$ is the box operator in curved spacetimes. When acting on a scalar quantity, it takes the form $\Box\Phi = \left[\partial_\nu \partial^\nu + \Gamma^\nu_{\nu\kappa} \partial^\kappa \right] \Phi$. Remembering that $\Gamma^\kappa_{\kappa\rho} = \frac{1}{\sqrt{-g}} \partial_\rho \sqrt{-g}$ (where $g < 0$ is the determinant of the metric) [14], the field equation can be written in the form

$$\left[\frac{1}{\sqrt{-g}} \partial_\kappa \left(g^{\kappa\rho} \sqrt{-g}\, \partial_\rho \right) - \mu^2 \right] \Phi = 0 \tag{1.3.4}$$

1.3.2 Schwarzschild background

Before diving into the Kerr spacetime, it is instructive to study the Klein-Gordon equation in the Schwarzschild background.

As we saw in §1.2.1, the metric determinant is $g = -r^4 \sin^2\theta$. Plugging this into (1.3.4) we get the master scalar field equation in Schwarzschild background

$$\begin{aligned} \frac{\partial}{\partial r} \left(r(r-2M) \frac{\partial \Phi}{\partial r} \right) - \frac{r^4}{r(r-2M)} \frac{\partial^2 \Phi}{\partial t^2} - \mu^2 r^2 \Phi + \\ + \frac{1}{\sin\theta} \frac{\partial}{\partial \theta} \left(\sin\theta \frac{\partial \Phi}{\partial \theta} \right) + \frac{1}{\sin^2\theta} \frac{\partial^2 \Phi}{\partial \phi^2} = 0 \end{aligned} \tag{1.3.5}$$

where we have rearranged the terms so as to display the separability of the equation. This form, along with the spherical symmetry and time independence of the metric, suggest the decomposition

$$\Phi = e^{-i\omega t} \hat{R}(r) A_{lm}(\theta, \phi) \tag{1.3.6}$$

Inserting this ansatz into the field equation, it separates into the following radial and angular part

$$r(r-2M) \frac{\partial}{\partial r} \left(r(r-2M) \frac{\partial \hat{R}}{\partial r} \right) + \left[\omega^2 r^4 - \left(\mu^2 r^2 + \lambda \right) r(r-2M) \right] \hat{R} = 0 \tag{1.3.7}$$

$$\sin\theta \frac{\partial}{\partial \theta} \left(\sin\theta \frac{\partial A}{\partial \theta} \right) + \lambda \sin^2\theta A + \frac{\partial^2 A}{\partial \phi^2} = 0 \tag{1.3.8}$$

where λ is the separation constant. With respect to the angular equation, further separation of variables dictates that $A(\theta, \phi) = e^{im\phi} Y_{lm}(\theta)$. Proceeding, we see that $Y_{lm}(\theta)$ satisfies the scalar spherical harmonics equation in four dimensions. This, of course, is not unexpected since we are dealing with a spherically symmetric problem. Imposition of regularity of the

spherical harmonics function Y_{lm} for all $\theta \in [0, \pi]$ gives that $\lambda = l(l+1)$ with l and $|m| \leq l$ being integers.

$$\sin\theta \frac{\partial}{\partial\theta}\left(\sin\theta \frac{\partial Y_{lm}}{\partial\theta}\right) + \left[l(l+1)\sin^2\theta - m^2\right] Y_{lm} = 0 \tag{1.3.9}$$

As for the radial equation, it can be written as a one-dimensional equation with an effective potential, i.e. Schröndinger form, by defining a new radial function R and a new radial variable x

$$R = \frac{\hat{R}}{r} \quad \text{and} \quad dx = \frac{r}{r-2M}dr \tag{1.3.10}$$

from which $x = r + 2M\ln(r-2M)$. Using these definitions, the radial equation takes the form

$$\frac{d^2R}{dx^2} + \left(\omega^2 - V\right) R = 0 \tag{1.3.11}$$

$$V(r) = \left(1 - \frac{2M}{r}\right)\left(\mu^2 + \frac{l(l+1)}{r^2} - \frac{2M}{r^3}\right) \tag{1.3.12}$$

Notice that in these coordinates, the Schwarzschild metric (1.2.1) takes the "nice" form

$$ds^2 = \left(1 - \frac{2M}{r(x)}\right)\left(-dt^2 + dx^2\right) + r^2(x)d\Omega_2^2 \tag{1.3.13}$$

The x coordinate is the natural choice for the definition of lightcone coordinates $t \pm x$. The simplification of the field equation into Schrödinger form is partly due to this choice.

1.3.3 Kerr background

We now proceed with deriving the scalar field equation in the Kerr background. The process is basically the same as in the Schwarzschild spacetime. However, the equations are now somewhat more complicated and great care is needed.

The metric determinant is now $g = -\rho^4\sin^2\theta = -\left(r^2 + a^2\cos^2\theta\right)^2\sin^2\theta$. Again, we insert this into (1.3.4) and after a considerable bit of algebra we get

$$\begin{aligned}&\frac{\partial}{\partial r}\left(\Delta\frac{\partial\Phi}{\partial r}\right) - \frac{a^2}{\Delta}\frac{\partial^2\Phi}{\partial\phi^2} - \frac{4Mra}{\Delta}\frac{\partial^2\Phi}{\partial\phi\partial t} - \frac{\left(r^2+a^2\right)^2}{\Delta}\frac{\partial^2\Phi}{\partial t^2} - \mu^2r^2\Phi + \\ &+\frac{1}{\sin\theta}\frac{\partial}{\partial\theta}\left(\sin\theta\frac{\partial\Phi}{\partial\theta}\right) + \frac{1}{\sin^2\theta}\frac{\partial^2\Phi}{\partial\phi^2} + a^2\sin^2\theta\frac{\partial^2\Phi}{\partial t^2} - \mu^2a^2\cos^2\theta\Phi = 0\end{aligned} \tag{1.3.14}$$

Again, we have grouped the terms such as to display the separability of the equation. In the Schwarzschild case, first, we separated the radial from angular part. Then, the angular function $A(\theta, \phi)$ naturally separated into $e^{im\phi}$ and Y_{lm}. This exponential is the appropriate eigenfunction for an axially symmetric geometry. We shall use it again as in [19] with the following ansatz

$$\Phi = e^{im\phi}e^{-i\omega t}R(r)\Theta(\theta) \tag{1.3.15}$$

Careful computation gives that with this ansatz, the field equation separates into the following two equations [7]

$$\frac{d}{dr}\left(\Delta\frac{dR}{dr}\right)+\frac{1}{\Delta}\left[a^2m^2-4Mram\omega+\left(r^2+a^2\right)^2\omega^2-\mu^2r^2\Delta\right]R=QR \tag{1.3.16}$$

$$\frac{1}{\sin\theta}\frac{d}{d\theta}\left(\sin\theta\frac{d\Theta}{d\theta}\right)+\left[-\mu^2a^2\cos^2\theta-a^2\omega^2\sin^2\theta-\frac{m^2}{\sin^2\theta}\right]\Theta=-Q\Theta \tag{1.3.17}$$

As far as the angular equation (1.3.17) is concerned, it can be brought into a more familiar form by redefining the separation constant $Q=\lambda_{ml}(-ic)+a^2\omega^2$.

$$\frac{1}{\sin\theta}\frac{d}{d\theta}\left(\sin\theta\frac{d\Theta}{d\theta}\right)+\left[c^2\cos^2\theta-\frac{m^2}{\sin^2\theta}\right]\Theta=-\lambda_{ml}\Theta\ ,\quad c^2=a^2\left(\omega^2-\mu^2\right) \tag{1.3.18}$$

This is the differential equation for the *oblate angular spheroidal function* $\Theta=S_{ml}\left(-ic,\cos\theta\right)$. λ_{ml} is its eigenvalue with $m\leq|l$ being integers. Again, as in the non-rotating case, such a solution for the angular part is expected since spheroidal functions correspond to problems of rotational symmetry such as this one. For more details see App. A.

1.3.4 Teukolsky's Radial Equation

It has been shown [20] that all field equations for scalar ($s=0$), vector ($s=\pm1$, i.e. electromagnetic) and tensor ($s=\pm2$, i.e. gravitational) perturbations in Kerr background are separable and yield differential equations with the same qualitative characteristics. They are summarized by *Teukolsky's master Radial Equation* (TRE)

$$\Delta^{-s}\frac{d}{dr}\left[\Delta^{s+1}\frac{dR_{slm}}{dr}\right]-V_sR_{slm}=0 \tag{1.3.19}$$

where R_{slm} is related to the actual field of spin s under study. The details of these relations are not directly related to this thesis and are thus not mentioned; they can be found in [20]. The potential V_s is given by

$$V_s=-\frac{1}{\Delta}\left[K^2+is\Delta'K-\Delta\left(2isK'+\lambda_{slm}\right)\right]\ ,\quad K=-(r^2+a^2)\omega+am\ ,\quad \mu=0 \tag{1.3.20}$$

The equations above show that the $s=0$ case presents us with the simplest version of the TRE. A source of complication is the explicit complex nature of the potential for $s\neq0$. As such, we have chosen to avoid such problems by studying the simple case of a scalar field knowing that the same approach can be applied to fields with $s\neq0$ with only minor modifications.

Note that the radial differential equations for both the Schwarzschild and the Kerr spacetimes are in agreement with the master radial equation [20] for $s=0$, $\mu=0$ (and $a=0$ for the Schwarzschild case).

[7] In eq.(5) of [19], the sign of μ^2 should be inverted and carried over to the rest of the publication.

CHAPTER 2

BTZ QNM: An exactly solvable model

Before studying problem of scalar QNM in 3+1 dimensions, it is instructive to look into a simpler problem where an exact solution is obtainable.

The BTZ solution was named after Banados, Teitelboim and Zanelli who discovered it [21]. It is (2+1) dimensional black hole solution to the Einstein equations with a negative cosmological constant (AdS). It has no angular momentum or electric charge. The only parameters on which it depends are the BH mass and the cosmological constant.

The AdS/CFT duality is directly applicable in the QNM of this spacetime as it yields the thermalization timescale in the dual two-dimensional CFT, which would otherwise be difficult to compute. What is more, it also serves as a toy model for one to get acquainted with the calculation of QNM.

2.1 BTZ metric

This spacetime's metric is given by

$$ds^2 = -f dt^2 + f^{-1} dr^2 + r^2 d\theta^2 \quad \text{with} \quad f = \frac{\left(r^2 - r_0^2\right)}{L^2} \tag{2.1.1}$$

Here, L is related to the cosmological constant $\Lambda = {}^{-1}/_{L^2}$ while the black hole's mass $M = {}^{r_0^2}/_{L^2}$. By inspection, one can see that the event horizon is a sphere of radius r_0.

2.2 The equation

Working in a spacetime with a non-zero cosmological constant means that the Ricci scalar is also non-zero. This allows us to introduce a minimal coupling with the scalar field tuned by $\tilde{\gamma}$ (the ${}^1/_8$ factor is there by convention).

$$\left[\frac{1}{\sqrt{-g}}\partial_\kappa \left(g^{\kappa\rho}\sqrt{-g}\,\partial_\rho\right) - \mu^2 - \frac{1}{8}\tilde{\gamma}R\right] X = 0 \tag{2.2.1}$$

Notice that since $R = -{}^{6}/_{L^2}$, the scalar mass μ can be absorbed into the coupling constant $\tilde{\gamma}$ (or the other way around) by the redefinition

$$\tilde{\gamma} \to \tilde{\gamma} + \frac{8}{6} L^2 \mu^2 \tag{2.2.2}$$

Consequently, with no loss of generality, we can set $\mu = 0$ and that is how we shall proceed. Due to spherical (in actuality circular!) symmetry, the following ansatz shall be used.

$$X(t, r, \theta) = e^{-i\omega t} \frac{\Psi(r)}{\sqrt{r}} Y_l(\theta) \tag{2.2.3}$$

where $Y_l = \exp(il\theta)$ denotes the 1-dimensional spherical harmonics. The extra factor of $1/\sqrt{r}$ is introduced for getting a better form of the equation. Working it out, indeed the differential equations for θ and r decouple and we get that Ψ obeys

$$\frac{\left(r^2 - r_0^2\right)^2}{L^4} \Psi'' + \frac{2}{L^4} r \left(r^2 - r_0^2\right) \Psi' + \left(\frac{\bar{A}}{r^2} + \bar{B} + \bar{C} r^2\right) \Psi = 0 \tag{2.2.4}$$

where

$$\tilde{A} = \frac{l^2 r_0^2}{L^2} + \frac{r_0^4}{4L^4} \tag{2.2.5}$$

$$\tilde{B} = -\frac{l^2}{L^2} + \omega^2 + \frac{r_0^2}{2L^4} + \frac{3\tilde{\gamma} r_0^2}{4L^4} \tag{2.2.6}$$

$$\tilde{C} = -\frac{3\left(\tilde{\gamma} + 1\right)}{4L^4} \tag{2.2.7}$$

In order to work with dimensionless quantities, we perform the following rescalings

$$r = x r_0 \quad \Rightarrow \quad \frac{d}{dr} \to \frac{1}{r_0} \frac{d}{dx} \quad \text{and} \quad \frac{d^2}{dr^2} \to \frac{1}{r_0^2} \frac{d^2}{dx^2} \tag{2.2.8}$$

$$A = \frac{\tilde{A}}{r_0^2} \frac{L^4}{r_0^2}, \quad B = \tilde{B} \frac{L^4}{r_0^2}, \quad C = \tilde{C} r_0^2 \frac{L^4}{r_0^2} \tag{2.2.9}$$

With this, we get that (2.2.4) becomes:

$$\left(x^2 - 1\right)^2 \Psi'' + 2x \left(x^2 - 1\right) \Psi' + \left(\frac{A}{x^2} + B + C x^2\right) \Psi = 0 \tag{2.2.10}$$

2.3 Solution

We want to bring this differential equation in a known form so that boundary conditions can be imposed. Its current structure suggests that $(x^2 - 1)$ and x might be good factors for an ansatz so we shall set $\Psi(x) = x^m \left(x^2 - 1\right)^n \Phi(x^2)$ and $z = x^2$, where m, n are left to be set later to what will be convenient. After a few algebraic manipulations (2.2.10) becomes

$$\Phi'' + \frac{Q_1(m,n) z - Q_0(m,n)}{z(z-1)} \Phi' + \frac{P_2(m,n) z^2 + P_1(m,n) z + P_0(m,n)}{z^2 (z-1)^2} \Phi = 0 \tag{2.3.1}$$

The primes denote differentiation with respect to z. The P_i's and Q_i's are given by

$$Q_0(m,n) = (2m+1)/2 \tag{2.3.2}$$
$$Q_1(m,n) = (3+2m+4n)/2 \tag{2.3.3}$$
$$P_0(m,n) = \left(A - m + m^2\right)/4 \tag{2.3.4}$$
$$P_1(m,n) = \left(B - 2m^2 - 2n - 4mn\right)/4 \tag{2.3.5}$$
$$P_2(m,n) = \left(C + m + m^2 + 2n + 4mn + 4n^2\right)/4 \tag{2.3.6}$$

2.3.1 The hypergeometric equation

The equation above looks quite similar to the hypergeometric differential equation (see App. B)

$$u''(z) + \frac{(\alpha+\beta+1)z - \gamma}{z(z-1)}u'(z) + \frac{\alpha\beta}{z(z-1)}u(z) = 0 \tag{2.3.7}$$

In order to bring our equation to this form we impose $P_0(m,n) = 0$ and $P_2(m,n) = -P_1(m,n)$ which give

$$m = \frac{1}{2}\left(1 \pm \sqrt{1-4A}\right) = \frac{1}{2}\left(1 \pm i\frac{2lL}{r_0}\right) \tag{2.3.8a}$$
$$\begin{aligned} n &= \pm\frac{i}{2}\sqrt{A+B+C} = \pm i\frac{L^2}{2r_0}\omega \\ &= \pm\frac{i\omega}{\omega_0}, \qquad \omega_0 = \frac{2r_0}{L^2} \end{aligned} \tag{2.3.8b}$$

Notice that (2.3.8) represent four separate set of solutions (m,n). Nevertheless, as it will be more evident later on, we of course expect them to yield identical results. As a result of the above, (2.3.1) reduces to

$$\Phi'' + \frac{Q_1(m,n)z - Q_0(m,n)}{z(z-1)}\Phi' + \frac{P_2(m,n)}{z(z-1)}\Phi = 0 \tag{2.3.9}$$

Comparison of the above with (2.3.7) yields that

$$\{\alpha,\beta\} = \frac{1}{2}\left(Q_1(m,n) - 1 \pm \sqrt{\left(Q_1(m,n)-1\right)^2 - 4P_2(m,n)}\right) \tag{2.3.10}$$
$$\gamma = Q_0(m,n) \tag{2.3.11}$$

As a result, the two complete and linearly independent solutions to (2.2.10) (see App. B) are

$$\Psi_1^+(x) = x^m(x^2-1)^n F\left(\alpha,\beta,1-\gamma+\alpha+\beta;\ 1-x^2\right) \tag{2.3.12a}$$
$$\Psi_2^+(x) = x^m(x^2-1)^n\left(1-x^2\right)^{\gamma-\alpha-\beta} F\left(\gamma-\alpha,\gamma-\beta,1+\gamma-\alpha-\beta;\ 1-x^2\right) \tag{2.3.12b}$$

2.4 Boundary conditions

As mentioned before, it is the boundary conditions that eventually select the set of quasi-normal modes. The former are expressed as functions of the tortoise coordinate r_*, the latter being defined so that the line element (2.1.1) takes the form $ds^2 = f\left(-dt^2 + dr_*^2\right) + r^2 d\theta^2$. This is achieved via $r_* = \int f^{-1} dr$ so that

$$r_*(x) = -\frac{L^2}{r_0} \tanh^{-1} x \quad \Longleftrightarrow \quad x(r_*) = -\tanh\left(\frac{r_0}{L^2} r_*\right) \tag{2.4.1}$$

2.4.1 Condition at the horizon

In the coordinates we have been using so far, the horizon is located at $r_* \to -\infty$ or equivalently $x = 1$. Remember that $F(\alpha, \beta, \gamma; 0) = 1$. This means that when investigating the leading behavior at this boundary, the hypergeometric functions can be omitted. At the horizon, only ingoing waves are permitted: [1]

$$\Psi_{in} \sim e^{-i\omega r_*} = \exp\left(\frac{i\omega}{\omega_0} \ln \frac{1+x}{1-x}\right) = \left(\frac{1+x}{1-x}\right)^{\frac{i\omega}{\omega_0}} \tag{2.4.2}$$

$$\sim (x-1)^{-\frac{i\omega}{\omega_0}} \tag{2.4.3}$$

with ω_0 given by (2.3.8b).

The leading terms of the two solutions at the horizon are

$$\Psi_1(x) \sim (x-1)^{\pm\frac{i\omega}{\omega_0}} \qquad \Psi_2(x) \sim (x-1)^{\mp\frac{i\omega}{\omega_0}} \tag{2.4.4}$$

It is now obvious that (2.3.8b) give linearly dependent solutions so that we are free to choose any n we prefer. We choose to keep n^- from (2.3.8b) so that our solution is given by (2.3.12a).

2.4.2 Condition at infinity

With the help of (B.2.6), (2.3.12a) can be expanded around infinity and yields

$$\Psi^{\infty}(x) = \frac{\Gamma(\alpha-\beta)\Gamma(1+\alpha+\beta-\gamma)}{\Gamma(\alpha)\Gamma(1+\alpha-\gamma)} x^{2n+m-2\beta} + \frac{\Gamma(\beta-\alpha)\Gamma(1+\alpha+\beta-\gamma)}{\Gamma(\beta)\Gamma(1+\beta-\gamma)} x^{2n+m-2\alpha} \tag{2.4.5}$$

We now calculate the exponents of x in the equation above and find that

$$2n^- + m - 2\beta = \frac{1}{2}\left(-1 - \sqrt{4+3\tilde{\gamma}}\right) \tag{2.4.6a}$$

$$2n^- + m - 2\alpha = \frac{1}{2}\left(-1 + \sqrt{4+3\tilde{\gamma}}\right) \tag{2.4.6b}$$

[1] $\tanh^{-1} x = \frac{1}{2} \ln\left(\frac{1+x}{1-x}\right)$

It is important to point out that we have *not yet chosen* either m^+ or m^-. Nevertheless, notice that in case $\tilde{\gamma} > -1$ the second term of (2.4.5) is divergent (since we're working in the $x \to \infty$ limit). By requiring that one of the arguments of the Γ functions in the denominator of the divergent term is a negative integer, we can get rid of the problem since $|\Gamma(-n)| = \infty$ for all positive integers n, i.e. $n \in \mathbf{N}$.

The frequencies for which this happens are termed *quasi-normal modes* of their generating equations are $\beta + n = 0$ and $1 + \beta - \gamma + n = 0$. For both $m^\pm$ these equations yield the same two solutions which can be summarized in

$$\boxed{\omega_n = \pm\frac{l}{L} - \frac{i}{4}\left(4n + 2 + \sqrt{4 + 3\tilde{\gamma}}\right)\omega_0 \ , \quad \omega_0 = \frac{2r_0}{L^2}} \tag{2.4.7}$$

Note that the solution we found is exact and so is the formula for the frequencies. An important feature they exhibit is characteristic for all black hole quasi-normal mode problems: they take the form $\omega_n = \pm l\delta_1 - i\,(\delta_2 + n\delta_3)$. The significance of this formula is that the real part of ω is proportional to the angular quantum number l. Moreover, the n dependence is all in the imaginary part.

Our result agrees with that found in [22] for $\tilde{\gamma} = 0$.

CHAPTER 3

WKB Approximation

3.1 WKB Approximation

The approximation method presented in this chapter, has been known for a very long time. It can be traced back to papers by Carlini, Liouville and Green. Its name is due to its rediscovery by **W**entzel, **K**rammers, **B**rillouin and **J**effreys this being the reason that it can also be found as the JWKB approximation. Most of the content of this chapter is derived and quoted from the wonderful work in [23].

The WKB approximation is a method for finding approximate solutions to linear differential equations with varying coefficients. The most general second order differential equation can always be recast in a form without a first-order term:

$$\epsilon^2 \frac{d^2\psi}{dx^2} + Q^2(x)\psi = 0 \tag{3.1.1}$$

The formal version of the method can be applied when ϵ is a "small" parameter. In this case, inserting the ansatz

$$\psi(x) = \exp\left\{\frac{1}{\epsilon}\int_{x_0}^{x} d\chi \sum_{n=0}^{\infty} y_n(\chi)\epsilon^n\right\} \tag{3.1.2}$$

in (3.1.1) and setting the coefficients of successive powers of ϵ equal to zero, we obtain the following set of equations:

$$y_0 = \pm iQ \tag{3.1.3}$$

$$\frac{dy_{n-1}}{dx} = -\sum_{m=0}^{n} y_m y_{n-m}\ , \quad n \geq 1 \tag{3.1.4}$$

It must be noted that this series solution is in general *not convergent but only asymptotic*.

Retaining in the expression for ψ only the first three terms in the exponent and using convenient normalization, we get the second order approximation

$$\psi(x) = \left(\frac{Q}{\epsilon}\right)^{-1/2} \exp\left\{\pm i \int_{x_0}^{x} \left(1 + \frac{\epsilon_0}{2}\right) \frac{Q}{\epsilon} d\chi\right\}, \quad \epsilon_0 = \left(\frac{Q}{\epsilon}\right)^{-3/2} \frac{d^2}{dx^2} \left(\frac{Q}{\epsilon}\right)^{-1/2} \tag{3.1.5}$$

The approximation (3.1.5) is valid if

$$\frac{1}{2} |\epsilon_0| \ll \frac{1}{2} \frac{d}{dx} \left(\frac{\epsilon}{Q}\right) \ll 1 \tag{3.1.6}$$

Moreover, if the further condition

$$\frac{1}{2} \left| \int_{x_0}^{x} \epsilon_0 \frac{Q}{\epsilon} d\chi \right| \ll 1 \tag{3.1.7}$$

is satisfied, one can still use the first-order approximation instead

$$\psi(x) = \left(\frac{Q}{\epsilon}\right)^{-1/2} \exp\left\{\pm i \int_{x_0}^{x} \frac{Q}{\epsilon} d\chi\right\} \tag{3.1.8}$$

Note that the choice of x_0 is arbitrary (it corresponds to a total multiplicative constant for the solution). From condition (3.1.7), it is noted that at any point x_0 the approximate solution (3.1.8) and its first derivative can be made to coincide with the the exact solution. The question is then how far one can move away from the point x_0 before the solution becomes inaccurate.

Note that even though we treat ϵ as small and use it as an expansion parameter, in all approximation formulas it always shows up through the ratio Q/ϵ and, as a result, it serves only as a formal mathematical tool.

3.2 Matrix WKB method

The method described in §3.1 carries the disadvantage of being an asymptotic formula. Nevertheless, an exact formula can be derived.

Consider the Schrödinger-like equation

$$\frac{d^2\psi}{dz^2} + Q^2(z)\psi = 0\,, \quad z \in \mathbb{C} \tag{3.2.1}$$

$Q^2(z)$ is a function which is analytic in a certain region of the complex z-plane. Also, appropriate cuts must be introduced to ensure its single-valuedness if needed.

As it stands, if $Q^2(z)$ was equal to 1, the solution would then be trivial. However, possible singularities and other intricacies of Q usually make this limit unattainable. Having said that, let us introduce new variables w, ϕ such that

$$\psi = \frac{\phi(z)}{\sqrt{q(z)}} \quad \text{and} \quad w(z) = \int^{z} q(\zeta) d\zeta \tag{3.2.2}$$

where $q(z)$ is at our disposal. This is the most general transformation that preserves the form of (3.2.1). The purpose of this transformation is to introduce an additional "degree of freedom" in our equation which we can tune to our needs. As a result, (3.2.1) becomes

$$\frac{d^2\phi}{dw^2} + (1+\epsilon)\,\phi = 0 \tag{3.2.3}$$

where the following definitions are equivalent

$$\epsilon(w) = \frac{Q^2 - q^2}{q^2} - q^{-1/2}\frac{d^2}{dw^2}\left(q^{1/2}\right) \tag{3.2.4a}$$

$$\epsilon(z) = \frac{Q^2 - q^2}{q^2} + q^{-3/2}\frac{d^2}{dz^2}\left(q^{-1/2}\right) \tag{3.2.4b}$$

If $q(z)$ is such that $\epsilon = 0$ then the solutions to (3.2.1) & (3.2.3) are given by

$$\phi(w) = \exp\{\pm iw\} \tag{3.2.5}$$

$$\psi(z) = q^{-1/2}\exp\left\{\pm i\int^z q(\zeta)d\zeta\right\} \tag{3.2.6}$$

respectively. As a result, we see that finding such $q(z)$ is equivalent to solving the initial problem. Of course, if the original problem is unsolvable, so will be this one. However, we have gotten closer to a solution.

Note that the first-order asymptotic solution (3.1.8) can be obtained by setting $q^2(z) = Q^2(z)$. This formula indicates that in many cases, one can obtain a function $\epsilon \sim 0$, i.e. not equal to zero but small enough. The aforementioned treatment gives the usual WKB approximation.

The matrix WKB approximation is a generalized version of this method which is based on different choices of $q(z)$ according to the $Q(z)$ function. Failure of the usual WKB approximation is usual around poles of the latter. This can be directly deduced from the form of ϵ in eqs. (3.2.4).

We require that ϵ remains small in the regions of the complex plane we are interested in and this leads to a choice of $q(z)$ which differs essentially from $Q(z)$. It is the art of this method for one to find an appropriate q. The definition of what "small" means in this context will be given shortly.

Assuming an appropriate choice of $q(z)$ has been made, we express ϕ as

$$\phi(w) = a_1(w)\exp(+iw) + a_2(w)\exp(-iw) \tag{3.2.7}$$

In regions where $\epsilon \sim 0$, the a_i's will be approximately constant. Since we have introduced *two* new independent functions we have the freedom to impose almost any condition we want between them. We choose this condition to be

$$\frac{da_1}{dw}\exp(iw) + \frac{da_2}{dw}\exp(-iw) = 0 \tag{3.2.8}$$

so that the first derivative of ϕ is

$$\frac{d\phi}{dw} = ia_1 \exp(iw) - ia_2 \exp(-iw) \tag{3.2.9}$$

as if a_i where constants (independent of w). Using (3.2.7), (3.2.8) and (3.2.9) we can write the original second order differential equation for ϕ, (3.2.5), as the following system of two first-order differential equations:

$$\frac{da_1}{dw} = \frac{1}{2} i\epsilon(w) \left\{a_1 + a_2 \exp(-2iw)\right\} \tag{3.2.10a}$$

$$\frac{da_2}{dw} = -\frac{1}{2} i\epsilon(w) \left\{a_2 + a_1 \exp(2iw)\right\} \tag{3.2.10b}$$

Introduce vectors $\mathbf{a}(w)$, $\mathbf{f}(w)$ and the matrix $\mathbf{M}(w)$:

$$\mathbf{a}(w) = \begin{pmatrix} a_1(w) \\ a_2(w) \end{pmatrix}, \quad \mathbf{f}(w) = \begin{pmatrix} \exp(+iw) \\ \exp(-iw) \end{pmatrix} \tag{3.2.11}$$

$$\mathbf{M}(w) = \frac{1}{2} i\epsilon(w) \begin{pmatrix} 1 & \exp(-2iw) \\ -\exp(2iw) & -1 \end{pmatrix} \tag{3.2.12}$$

Note that, by simple inspection, $\mathbf{M}(w)$ is singular and traceless. With these at hand, the solution (3.2.7) reads $\phi(w) = \mathbf{a}(w)\mathbf{f}(w)$ and the system (3.2.10) can be written in the compact form $\mathbf{a}' = \mathbf{M}(w)\mathbf{a}$, where the prime denotes differentiation with respect to w. The vector differential equation can also be written in the integral form

$$\mathbf{a}(w) = \mathbf{a}(w_0) + \int_{w_0}^{w} dw_1 \mathbf{M}(w_1)\mathbf{a}(w_1) \tag{3.2.13}$$

By working iteratively, the solution of the above integral equation is

$$\mathbf{a}(w) = \mathbf{F}(w, w_0)\mathbf{a}(w_0) \tag{3.2.14}$$

where the matrix $\mathbf{F}$ is given by the infinite sum

$$\begin{aligned} \mathbf{F}(w, w_0) = 1 &+ \int_{w_0}^{w} dw_1 \mathbf{M}(w_1) \\ &+ \int_{w_0}^{w} dw_1 \mathbf{M}(w_1) \int_{w_0}^{w_1} dw_2 \mathbf{M}(w_2) \\ &+ \int_{w_0}^{w} dw_1 \mathbf{M}(w_1) \int_{w_0}^{w_1} dw_2 \mathbf{M}(w_2) \int_{w_0}^{w_2} dw_3 \mathbf{M}(w_3) \\ &+ \dots \end{aligned} \tag{3.2.15}$$

These expressions give the general solution to our differential equation. It can be shown [23] that in any region of the complex w-plane where the integral

$$\int_{w_0}^{w} \left| m(w')dw' \right| \quad \text{assuming} \quad m(w) : \quad \sum_j |M_{ij}(w)| \leq m(w) \tag{3.2.16}$$

along a conveniently chosen path from w_0 to w is bounded, the series (3.2.15) converges. Of course, the contours of corresponding integrals must be chosen appropriately so that they stay within the analytic region of **M**.

Since ϵ is expected to be small for this approximation to be valid, it is evident that it should also capture a measure of its error. Let us define a function τ such that

$$\tau = \int_{w_0}^{w} \left|\epsilon(w')dw'\right| \tag{3.2.17}$$

This quantity shall prove useful later on in calculating both errors (in terms of $O(\tau)$ symbols) and upper bounds in our estimates.

3.3 Properties of the F matrix

The formalism presented here possesses extremely rich properties and relations. It is not the purpose of this thesis to comprehensively list them all or give their proofs. In this section, we shall only present the ingredients necessary for the analysis done in later chapters along with some intuitive arguments for their validity. The interested reader is encouraged to consult [23].

Firstly, let us present some general properties. Multiplying (3.2.15) by **M** and integrating term-by-term we get that the **F** matrix satisfies the integral equation $\mathbf{F}(w, w_0) = 1 + \int_{w_0}^{w} dw' \mathbf{M}(w')\mathbf{F}(w', w_0)$ from which it follows that

$$\frac{\partial \mathbf{F}(w, w_0)}{\partial w} = \mathbf{M}(w)\mathbf{F}(w, w_0) \tag{3.3.1}$$

As a result, [1] we get that $[\det\mathbf{F}(w, w_0)]' = 0$ and hence **F**'s determinant is independent of w. Furthermore, by its definition (3.2.15) it is evident that for $w = w_0$, **F** is a unit matrix. Consequently, we have that

$$\det\mathbf{F}(w, w_0) = 1 \tag{3.3.2}$$

Noting from (3.2.14) that $\mathbf{F}(w_0, w) = [\mathbf{F}(w, w_0)]^{-1}$, by direct matrix inversion we thus get

$$\begin{pmatrix} F_{11}(w_0, w) & F_{12}(w_0, w) \\ F_{21}(w_0, w) & F_{22}(w_0, w) \end{pmatrix} = \begin{pmatrix} F_{22}(w, w_0) & -F_{12}(w, w_0) \\ -F_{21}(w, w_0) & F_{11}(w, w_0) \end{pmatrix} \tag{3.3.3}$$

Moreover, **F** admits to the multiplication rule

$$\mathbf{F}(z_0, z_2) = \mathbf{F}(z_0, z_1)\mathbf{F}(z_1, z_2) \tag{3.3.4}$$

Our interest lies in having explicit formulas for the matrix **F** connecting arbitrary points in the complex plane. Complications arise due the definition (3.2.4) of ϵ since it is evident that $\epsilon \gg 0$ around poles and singularities of $q^2(z)$; a fact that has already been pointed out.

[1] remember that $(\det\mathbf{F})' = \det\mathbf{F}\mathrm{tr}\left(\mathbf{F}^{-1}\mathbf{F}'\right)$

3.4 Estimates for the connection matrix $\mathbf{F}$, $\mathbb{R}$eal $Q^2(x)$

The connection formulas to be presented will not be accompanied by their respective proofs as it is not the purpose of this thesis. Nevertheless, a few words about their derivation are in order.

It appears that there is much simplification if we assume that both $q^2(z)$ and $Q^2(z)$ are real on the real axis, x. In such a case, the differential equation (3.2.1) is invariant under complex conjugation. This means that if $\psi(x)$ is a solution on the real axis, then so is $\psi^*(x)$. This property can be taken advantage of to derive relations between different components of the connection matrix. These help in the derivation of explicit formulas for $\mathbf{F}$.

It will henceforth be assumed that the complex plane is appropriately cut so that $q^2(z)$ is analytic and single valued. All paths of integration used are assumed to not cross any such cuts.

3.4.1 General considerations

First, let us introduce some useful terminology already adopted in the literature. We shall separate the real axis into regions according to the sign of $q^2(x)$. Regions of positive sign are called "classically allowed" while regions of negative sign are called "classically forbidden". Last but not least, zeros of $q^2(x)$ are also called "classical turning points".

The reason behind these naming conventions lies in the original WKB approximation where q^2 is set equal to Q^2. Starting with a Schrödinger equation where $Q^2 = E - V$, the terminology used does indeed carry physical meaning.

For x_1, x_2 two points on the real axis, the reality of $Q^2(x)$ can be shown [23] to imply the symmetry relation

$$\mathbf{F}(x_1, x_2) = \mathbf{B}(x_1)\mathbf{F}^*(x_1, x_2)\mathbf{B}^*(x_2) \tag{3.4.1}$$

where the asterisk denotes complex conjugation and the matrix $\mathbf{B}$ is given by

$$\mathbf{B}(x) = \frac{q(x)}{|q(x)|}\begin{pmatrix} 0 & \exp\left[2\Im w(x)\right] \\ \exp\left[-2\Im w(x)\right] & 0 \end{pmatrix} \qquad \text{if} \quad q^2(x) > 0 \tag{3.4.2a}$$

$$\mathbf{B}(x) = \frac{q(x)}{|q(x)|}\begin{pmatrix} \exp\left[-2i\Re w(x)\right] & 0 \\ 0 & \exp\left[2i\Re w(x)\right] \end{pmatrix} \qquad \text{if} \quad q^2(x) < 0 \tag{3.4.2b}$$

Relations between different components of the connection matrix derived from (3.4.1) are of importance for work to be done in the following chapters. Wherever there is no risk of confusion, we shall omit the arguments of the $\mathbf{F}$ matrix; essentially, $\mathbf{F}_{ij} = \mathbf{F}_{ij}(x_1, x_2)$.

There are many cases for which the connection matrix can be derived. Here, we will only give the ones relevant to this thesis.

3.4.2 Two points in the same classically allowed region

This is the case when both x_1 and x_2 belong in the same classically allowed region, i.e. $q^2(x_i) > 0$ and there is no cut or pole between them. Then, along the interval (x_1, x_2) the function $w(x)$ is real and the phase of $\sqrt{q(x)}$ is constant.

Symmetry relations (3.4.1) and (3.4.2) simplify to

$$F_{22} = F_{11}^* \quad \text{and} \quad F_{12} = F_{21}^* \tag{3.4.3}$$

With these in mind, the condition of the matrix having a unit determinant, eq.(3.3.2), now reads

$$|F_{11}| - |F_{21}| = 1 \tag{3.4.4}$$

The integration contour that arises naturally is the path connecting the two points along the real line. With these considerations, the following estimates can be shown [23] to hold

$$|F_{11} - 1| \leq \frac{1}{2}\left(e^{\tau} - 1\right) \tag{3.4.5a}$$

$$|F_{21}| \leq \frac{1}{2}\left(e^{\tau} - 1\right) \tag{3.4.5b}$$

Relations with respect to the rest of the matrix components can be derived by the symmetry relations and the estimates above. As a result, for small enough values of τ, the connection matrix is approximately equal to the unit matrix.

This is an important result. It shows that if we are far away from any roots or poles of the potential, so that $\epsilon \sim 0$, the $\mathbf{a}$ vector remains constant (which is, of course, intuitively expected).

3.4.3 Two points on opposite sides of a classical turning point

We shall now study the slightly more complicated case of the two points being on opposite sides of a classical turning point. This root of q^2 is assumed to be of the first order. We choose x_1 to lie on the classically forbidden region, i.e. $q^2(x_1) < 0$ and x_2 on the classically allowed, $q^2(x_2) > 0$.

With respect to the relation between x_1 and x_2 and the phase of $\sqrt{q(z)}$, we differentiate between the following

$$x_1 < x_2 \quad \text{and} \quad q(x_1)^{1/2} = e^{i\pi/4}\sqrt{|q(x_1)|}\,, \quad q(x_2)^{1/2} = \sqrt{|q(x_2)|} \tag{3.4.6a}$$

$$x_1 > x_2 \quad \text{and} \quad q(x_1)^{1/2} = \sqrt{|q(x_1)|}\,, \quad q(x_2)^{1/2} = e^{-i\pi/4}\sqrt{|q(x_2)|} \tag{3.4.6b}$$

The two cases above can be treated simultaneously the only difference being some signs. In the following formulas, the upper sign shall denote case (3.4.6a) while the lower one (3.4.6b).

The complex z-plane is assumed to be cut along the real line and the function $\sqrt{q(z)}$ is defined on and above the real axis. For the definition (3.2.2) of $w(z)$, choose the lower bound of the

integral to be the turning point x' lying between the x_i's and as a result, $w(x') = 0$. The symmetry relations now take the form

$$F_{12} = \pm i F_{11}^* \quad \text{and} \quad F_{21} = \pm i F_{22}^* \tag{3.4.7}$$

while the determinant condition takes the form

$$F_{11}F_{22} + F_{11}^* F_{22}^* = 1 \tag{3.4.8}$$

Since ϵ (and thus τ) diverge on the turning point, the path of integration can no longer be the whole real line segment (x_1, x_2). Instead, the root x' shall be avoided by passing around it in a semi-circle through the complex z-plane. We still stay on the real axis everywhere else though.

Complementary to the root being of the first-order, it must also lie sufficiently far from other zeros and poles of $q^2(z)$ so that $|\exp\{iw(z)\}|$ has a single extremum on this semi-circle.

Under these assumptions, the following estimates hold

$$|F_{11} - 1| \leq \tau + O\left(\tau^2\right) \tag{3.4.9a}$$

$$|F_{22}| \leq \left|e^{2iw(x_1)}\right| \left(\frac{\tau}{2} + O\left(\tau^2\right)\right) \tag{3.4.9b}$$

The factor $|\exp\{2iw(x_1)\}|$ appearing in the latter of these estimates increases rapidly as x_1 moves away from the turning point x'. The elements F_{22} and F_{21} vary strongly and remain practically undetermined.

On the other hand, the values of F_{11} and F_{12} remain accessible.

$$F_{11} \simeq 1 + O(\tau) \quad \text{and} \quad F_{12} \simeq \pm\left[i + O(\tau)\right] \tag{3.4.10}$$

It is instructive to derive the connection formulas in one extra case. We shall now take the lower bound of the $w(z)$ integral (3.2.2) to be equal to $x'' < x_1$. Following the notation of (3.4.6), the case we are studying now is

$$x_1 < x_2 \quad \text{and} \quad q(x_1)^{1/2} = \exp\left(-i\pi/4\right)\sqrt{|q(x_1)|}\,, \quad q(x_2)^{1/2} = -i\sqrt{|q(x_2)|} \tag{3.4.11}$$

With these assumptions, the symmetry relations now read

$$F_{12} = iF_{11}^* e^{-2K(x'')} \quad \text{and} \quad F_{21} = iF_{22}^* e^{2K(x'')} \tag{3.4.12}$$

where K is given by

$$K(x) = \int_x^{x'} |q(y)|\, dy \tag{3.4.13}$$

The condition of the determinant being equal to one takes the same form as in (3.4.8). Again, we have the same considerations as before relating to the integration contour. The estimates now are

$$|F_{11}| \leq e^{2K(x_1)} \left(\frac{\tau}{2} + O\left(\tau^2\right) \right) \tag{3.4.14}$$

$$|F_{22} - 1| \leq \tau + O\left(\tau^2\right) \tag{3.4.15}$$

As before, the factor $\exp[2K(x_1)]$ increases rapidly as x_1 moves away from x' so that the estimate above makes F_{11} and F_{12} practically indeterminable. However, the rest of the components remain well approximated and for small enough τ are found to be

$$F_{22} \simeq 1 + O(\tau) \quad \text{and} \quad F_{21} \simeq e^{2K(x'')} \left[i + O(\tau) \right] \tag{3.4.16}$$

Notice that, with respect to the determinability of the whole connection matrix, the situation is reversed in comparison to the previous case. It is now the F_{11} and F_{12} that are inaccessible via this method while F_{22} and F_{21} are not.

3.4.4 Two points on opposite sides of a potential barrier

The next case study is that of two points x_1, x_2, both in a classically allowed region but separated by a classically forbidden region marked by the simple[2] classical turning points $x' < x''$. As for the lower limit of the $w(z)$ definition integral, it is fixed to be the turning point x'.

We take x_i's such that $x_1 < x_2$ and assumed to lie far enough from the turning points so that the original WKB approximation may be used in their respective neighbourhoods. As noted earlier, this analysis is dependent on choosing a path, Λ, so that the τ integral (3.2.17) remains small compared to 1. This results in two distinctive cases depending on the "proximity" of the two turning points. We shall treat them separately.

The first shall be when the potential barrier is such that x', x'' are sufficiently far away so Λ can be a straight line joining the x_i's while circling the turning points when close to their vicinity.

The second case is when the turning points are close enough so that they have to be circled by the same (i.e. one and only) semi-circle contour in order for the τ integral to remain well smaller than 1. In both cases, it is assumed that there is a point $z_0 \in \Lambda$ such that $|\exp\{iw(z)\}|$ has a single minimum in $(x_1, z_0) \in \Lambda$ and a single maximum in $(z_0, x_2) \in \Lambda$.

We cut the z-plane along the real axis and consider the function $\sqrt{q(z)}$ on and above it. The choice of its phase on the line segment $[x_1, x_2]$ shall be

- $x \in (x_1, x')$: $q(x)^{1/2} = \sqrt{|q(x)|}$
- $x \in (x', x'')$: $q(x)^{1/2} = \exp\left\{-i\frac{\pi}{4}\right\} \sqrt{|q(x)|}$

[2] i.e. first order

- $x \in (x'', x_2)$: $q(x)^{1/2} = -i\sqrt{|q(x)|}$

We shall also need the quantity K which, similarly to before, is defined as

$$K = \int_{x'}^{x''} |q(z)|dx = i \int_{x'}^{x''} q(z)dx \tag{3.4.17}$$

The symmetry relations and the determinant condition read

$$F_{11} = -F_{22}^* e^{2K} \quad \text{and} \quad F_{21} = -F_{12}^* e^{2K} \tag{3.4.18a}$$

$$|F_{12}|^2 - |F_{22}|^2 = e^{-2K} \tag{3.4.18b}$$

Case 1: Farly lying turning points

Combining the approaches presented previously, it can be shown that the connection matrix has the following structure

$$\mathbf{F} \simeq \begin{pmatrix} -e^{2K}\left[1 + O(\tau)\right] & i + O(\tau) \\ e^{2K}\left[i + O(\tau)\right] & 1 + O(\tau) \end{pmatrix} \tag{3.4.19}$$

Case 2: Closely lying turning points

In this case, the connection matrix can be approximated by

$$\mathbf{F} \simeq \begin{pmatrix} -e^{2K}\left[1 + O(\tau)\right] & \sqrt{1 + e^{-2K}}\left[i + O(\tau)\right] \\ e^{2K}\sqrt{1 + e^{-2K}}\left[i + O(\tau)\right] & 1 + O(\tau) \end{pmatrix} \tag{3.4.20}$$

Notice that the difference between the two formulae is significant only when $e^{-2K} \gg \tau$. In principle, this is the case when the turning points lie close to each other.

3.5 Estimates for the connection matrix $\mathbf{F}$, $\mathbb{C}$omplex $Q^2(z)$

In the previous section, we examined the form of the connection matrix $\mathbf{F}$ under the assumption that $Q^2(z)$ is real on the $x = \Re(z)$ axis. We presented estimates for various cases of the points to be connected according to which regions they were into. The estimates to be presented in this section will be useful for the implementation *monodromy method*. For that, we shall need to take a slightly different approach.

First of all, we need not restrict ourselves to cases where $Q^2(z)$ is real on the real axis. We will present the $\mathbf{F}$ matrix connecting certain classes of points around a well isolated zero of $Q^2(z)$.

3.5.1 Stokes' and anti-Stokes' lines

In all subsequent cases of this section, we set the lower bound of the $w(z)$ definition integral (3.2.2) to be the zero or pole itself. From this point, there emerge certain lines (in the complex z-plane) on which $w(z)$ is purely imaginary and other ones on which it is purely real. We thus define the following:

$$\textbf{Stokes' lines:} \quad w(z) \in \mathbb{I} \Leftrightarrow \Re w(z) = 0 \tag{3.5.1a}$$

$$\textbf{anti-Stokes' lines:} \quad w(z) \in \mathbb{R} \Leftrightarrow \Im w(z) = 0 \tag{3.5.1b}$$

As it turns out, there are interesting properties related to these lines. They come in pairs, i.e. there is always a Stokes' line in between every two anti-Stokes' line. From an n^{th} order zero of $q^2(z)$, there emerge $n+2$ Stokes' and $n+2$ anti-Stokes lines.

It can be shown [23] that for two points z_1, z_2 lying on the same anti-Stokes' line, both far from the zero so that $\tau \ll 1$, we have $\mathbf{F}(z_1, z_2) \simeq \mathbb{I}_2$. In what follows, we shall present the approximate form of the $\mathbf{F}$ matrix when connecting points on different anti-Stokes' lines.

3.5.2 Region around a first order zero of $Q^2(z)$

Let us assume $Q^2(z)$ has a zero of the first order well isolated from its other zeros or poles. Without loss of generality we may assume that this zero occurs at $z = 0$. We set $q^2(z)$ equal to $Q^2(z)$ and, consequently, we are going to use them interchangeably in this subsection. As mentioned earlier, the lower part of the $w(z)$ integral is set equal to 0, i.e. the point where $Q^2(z) = 0$.

From the definition (3.2.2) of $w(z)$, we have that $w(z) \sim z^{3/2} + O\left(z^{5/2}\right)$. Consistently with our statement above, there are 3 Stokes' and 3 anti-Stokes' lines emerging from z_0. We cut the complex plane along one of the anti-Stokes' lines. This choice imposes such a phase for $q(z)$ so that it has opposite signs on opposite sides of the chosen anti-Stokes' line.

Starting infinitesimally on the right of the cut and proceeding in an anticlockwise manner, we define the points $z_0, \ldots, z_6$ such that

- z_1, z_3, z_5 lie on consecutive Stokes' lines
- z_0, z_2, z_4, z_6 lie on consecutive anti-Stokes' lines with z_0, z_6 infinitesimally close to each other but on opposite side sides of the cut, essentially on two successive Riemann sheets.
- they all lie sufficiently far from 0, the root of $q^2(z)$ so that $\tau \ll 1$ along a path connecting them.

Utilizing the fact that any solution to our original differential equation (3.2.1) should be one-valued around a root of $Q^2(z)$, it can be shown that

$$\mathbf{F}(z_0, z_6) = \begin{pmatrix} 0 & -i \\ -i & 0 \end{pmatrix} \tag{3.5.2}$$

Note that this is an exact formula. Using the group property (3.3.4) of the $\mathbf{F}$ matrix, it can also be shown that

$$\mathbf{F}(z_2, z_0) \simeq \begin{pmatrix} 1 & i \\ 0 & 1 \end{pmatrix}, \quad \mathbf{F}(z_4, z_2) \simeq \begin{pmatrix} 1 & 0 \\ i & 1 \end{pmatrix}, \quad \mathbf{F}(z_6, z_4) \simeq \begin{pmatrix} 1 & i \\ 0 & 1 \end{pmatrix} \tag{3.5.3}$$

where we have omitted $\mathrm{O}(\tau)$ terms.

3.5.3 Stokes' phenomenon

Intuitively, the estimates (3.5.3) give the approximate changes in behavior that take place in the solution to our original differential equation when going from one anti-Stokes' line to the next one by *crossing a Stokes' line*.

Notice that these connection matrices have off-diagonal elements. Their structure presents the ability for some solutions to completely change their behavior per region of the complex plane. Exponentially small or large terms can be switched on and off by crossing a Stokes' line.

Essentially, we find the set of solutions of a differential equation to be multivalued around one or more points. However, the coefficients of the equation are entire functions around these points and so the complete solution should be as well. Since we are approximating a locally single-valued solution by locally multivalued functions, the approximation can only be domain-dependent. [24] This constitutes the *Stokes phenomenon*.

3.6 Quasi-normal modes and the WKB approximation

The use of the WKB approximation for problems related to quasi-normal modes is motivated by the similarity between Schrödinger's equation and perturbation field equations in black hole backgrounds.

As is, the nature of finding the quasi-normal modes ω_n constitutes an eigenvalue problem of the Schrödinger type where, as seen in §1.3, the potential $V(r)$ of the equation is a complicated expression that depends on the specifics of the spacetime. Moreover, in some spacetimes e.g. Kerr, the potential *also* depends on the eigenvalue itself i.e. the QNM ω_n.

The complicated nature of this potential is what makes the problem difficult to attack. Its wide variations make a global WKB approximate solution impossible. Nevertheless, there is an alternate route.

The procedure starts by separating spacetime in successive regions where the "original" WKB method can be applied. After computing the separate solutions, one carefully matches them across their respective boundaries. It is the imposition of the "outer" boundary conditions (i.e. at the horizon and at infinity) that will provide us with the allowed values for ω_n, the *quasi-normal modes*.

Essentially, the WKB method for computing QNMs involves propagating a solution valid at the horizon (a purely ingoing wave) through a complicated potential defined by the nature of the spacetime to infinity where one constrains the modes, i.e. ω_n, so that *only* outgoing waves are allowed.

It is here that the matrix WKB method comes in handy. The result can be obtained by the product of $\mathbf{F}$ matrices computed for separate regions of the potential. We then use the group property of the connection matrix, $\mathbf{a}(-\infty) = \mathbf{F}(-\infty, +\infty)\,\mathbf{a}(+\infty)$. The quasi-normal generating equation then is found by requiring that the appropriate part of the connection matrix is zero. For a similar approach see [25].

3.6.1 Ansatz

In order to begin tackling the problem, we first have to bring our differential equation into Schrödinger form. To do that, let us introduce a *tortoise* coordinate x and the additional ansatz u

$$u = \sqrt{r^2 + a^2}R, \qquad dx = \frac{r^2 + a^2}{\Delta}dr \tag{3.6.1}$$

With these, $r \in (r_+, \infty)$ maps to $x \in (-\infty, \infty)$. The radial scalar field equation (1.3.16) reduces to

$$\frac{d^2u}{dx^2} + Q^2(x)u = 0 \tag{3.6.2}$$

$$\begin{aligned} Q^2(x) = \omega^2 &+ \frac{\Delta\mu^2}{r^2 + a^2} \\ &- \frac{4Mram\omega - a^2m^2 + \Delta\left[\lambda_{ml}(-ic) + c^2\right]}{\left(r^2 + a^2\right)^2} \\ &- \frac{\Delta\left(3r^2 - 4Mr + a^2\right)}{\left(r^2 + a^2\right)^3} \\ &+ \frac{3\Delta^2 r^2}{\left(r^2 + a^2\right)^4} \end{aligned} \tag{3.6.3}$$

in agreement with [19]. Remember that $c^2 = a^2\left(\omega^2 - \mu^2\right)$.

As explained in §3.2, we shall introduce new variables such that the equation keeps its current form (no 1st order term) while ϵ will be close to zero. Here lies one of the reasons for using transformation (3.6.1). Setting $q^2 = Q^2$ achieves a measure of ϵ which is much less than one.

This analysis depends vitally on the number of zeros $Q^2(x)$ has. Let us note that

$$Q^2(-\infty) = \left(\omega - \frac{mr_-}{2aM}\right)^2, \quad Q^2(\infty) = \omega^2 - \mu^2 \tag{3.6.4}$$

3.6.2 Boundary conditions

As mentioned before, the boundary conditions we want are waves which are ingoing at the horizon and outgoing at infinity. Starting at spatial infinity, purely outgoing waves means $\mathbf{a}(\infty) \sim (0, 1)$.

At the horizon, things are a bit more complicated. The solutions are linear combinations of $\exp\left[\pm i\left(\omega - \frac{mr_-}{2aM}\right)x\right]$. Care must be taken in order to assess which solution is ingoing and which one is outgoing. We distinguish between the two following cases

$$\begin{array}{lll} \Re\{\Omega\} < 0 & \Rightarrow & \mathbf{a}(-\infty) \sim (0,1) \\ \Re\{\Omega\} > 0 & \Rightarrow & \mathbf{a}(-\infty) \sim (1,0) \end{array} \quad \text{where} \quad \Omega = \omega - \frac{mr_-}{2aM} \tag{3.6.5}$$

The QNM generating equations then are

$$\Re\{\Omega\} < 0 \quad \Rightarrow \quad F_{12}(\pm\infty, \mp\infty) = 0 \tag{3.6.6a}$$

$$\Re\{\Omega\} > 0 \quad \Rightarrow \quad F_{22}(-\infty, \infty) = 0 \quad \Leftrightarrow \quad F_{11}(\infty, -\infty) = 0 \tag{3.6.6b}$$

Initially, we shall assume that ω is real and apply the estimates of §3.4. It is later on that we analytically continue to complex frequencies. It has to be pointed out that this assumption is not explicit in [25] (where part of this thesis is based) as well as other works in this field. Even though we cannot find adequate mathematical reasoning that supports it we shall still follow through with it.

Numerical analysis for various values of the parameter set shows that the potential has from zero to three turning points. Consequently, we shall deal with these situations only.

3.6.3 One turning point

Let us first start by assuming that the potential has only one zero outside the black hole horizon. This, as well as any treatment with an odd number of turning points, requires that $\omega^2 < \mu^2$.

We studied this case in §3.4.3 and shall follow accordingly. It was argued that the $\mathbf{F}(+\infty, -\infty)$ matrix can only be partially determined in this case as the F_{22} and F_{21} elements are wildly varying. However, this is no problem as it is the two other elements that are of interest to us.

The formulas in (3.4.10) show that, assuming our approximation is valid i.e. $\tau \to 0$, conditions (3.6.6) cannot be satisfied since F_{11} and F_{12} are of O(1). As a result, the quasi-normal frequencies ω have to be such that the potential Q has more than one turning points.

3.6.4 Two turning points

Let us now assume that the potential has only two zeros in the region *outside* the black hole. This translates to $\omega^2 > \mu^2$.

We saw in §3.4.4 that the connection matrix depends on the proximity of the two turning points. At the end of the same section, though, it was argued that by assuming they are close (i.e. taking the appropriate integration contour) still yields the correct result by virtue of the extra terms being negligible in case the roots turn out to be far after all.

Let the two turning points be $x_1,\ x_2$. We define the phase of $q(z)^{1/2}$ and the necessary integration contours as in §3.4.4. The connection matrix is approximated by (3.4.20) which

we rewrite here with $\mathrm{O}(\tau)$ terms dropped, i.e. $\tau \ll 1$.

$$\mathbf{F}(-\infty,\infty) \simeq \begin{pmatrix} -e^{2K_{12}} & i\sqrt{1+e^{-2K_{12}}} \\ ie^{2K_{12}}\sqrt{1+e^{-2K_{12}}} & 1 \end{pmatrix}, \quad K_{12} = \int_{x_1}^{x_2} |q(z)|dz = i\int_{x_1}^{x_2} q(z)dz \tag{3.6.7}$$

Condition (3.6.6a) yields $e^{-2K_{12}} + 1 = 0$ or equivalently

$$\int_{x_1}^{x_2} q(z)dz = -\pi\left(n + \frac{1}{2}\right) \tag{3.6.8}$$

It is interesting to notice that condition (3.6.6b) cannot be satisfied under the current assumptions since $F_{22}(-\infty,\infty) = 1$. This enforces that $\Re(\omega) < \frac{mr_-}{2aM}$.

3.6.5 Three turning points

Last but not least, let Q^2 (and thus q^2) have three roots in the region outside the black hole. As mentioned before,§3.6.3 requires $\omega^2 < \mu^2$.

The roots shall be denoted by $x_1,\ x_2$ and x_3. Space is naturally divided into four regions. We enumerate them along with the choice of phase for $q^{\frac{1}{2}}$.

$$\begin{array}{rlll} \mathrm{I}: & x \in (-\infty,\ x_1), & q^2(x) > 0 \quad \text{and} & q(x)^{1/2} = -i\sqrt{|q(x)} \\ \mathrm{II}: & x \in (x_1,\ x_2), & q^2(x) < 0 \quad \text{and} & q(x)^{1/2} = \exp\left\{-i\tfrac{\pi}{4}\right\}\sqrt{|q(x)|} \\ \mathrm{III}: & x \in (x_2,\ x_3), & q^2(x) > 0 \quad \text{and} & q(x)^{1/2} = \sqrt{|q(x)|} \\ \mathrm{IV}: & x \in (x_3,\ \infty), & q^2(x) < 0 \quad \text{and} & q(x)^{1/2} = \exp\left\{-i\tfrac{\pi}{4}\right\}\sqrt{|q(x)|} \end{array} \tag{3.6.9}$$

With this choice of phases, we have that $\mathbf{F}(\mathrm{III},\mathrm{I})$ is given by (3.6.7) (i.e. (3.4.20)) with the substitution $K_{12} \to K_{21}$. Remember that the lower bound of the w-integral is in this case set to be the turning point x_2

In section §3.4.3 we calculated the connection matrix appropriate for the $(\mathrm{III},\mathrm{IV})$ regions. It is given by

$$\mathbf{F}(\mathrm{IV},\mathrm{III}) = \begin{pmatrix} 1+\mathrm{O}(\tau) & -i+\mathrm{O}(\tau) \\ \text{ind.} & \text{ind.} \end{pmatrix} \tag{3.6.10}$$

where ind. signifies the indeterminacy of the corresponding elements due to their strongly varying nature. Further on, we remind the reader that for this connection matrix to be valid, the lower bound of the w-integral must be set to be the turning point x_3.

With these in mind, the connection matrix $\mathbf{F}(\infty,-\infty) = \mathbf{F}(\mathrm{IV},\mathrm{I})$ can be calculated through to matrix product

$$\mathbf{F}(\mathrm{IV},\mathrm{I}) = \mathbf{F}(\mathrm{IV},\mathrm{III}) \cdot \mathbf{\Phi}(x_2,\ x_3) \cdot \mathbf{F}(\mathrm{III},\mathrm{I}) \tag{3.6.11}$$

where the phase matrix $\mathbf{\Phi}$ is given by

$$\mathbf{\Phi}(x_2,\ x_3) = \mathrm{diag}\left[\exp(i\phi), \exp(-i\phi)\right], \quad \phi = \int_{x_3}^{x_2} q(z)dz = K_{32} \tag{3.6.12}$$

and represents the phase shift introduced by changing the lower bound of the w integral from x_3 to x_2 in order for the connection matrix $\mathbf{F}(\mathrm{IV}, \mathrm{III})$ to be applicable. The phase shift is equal to K_{32} because $q(z) > 0$ for $x \in (x_2, x_3)$, see (3.6.9).

Due to the aforementioned, with $\mathrm{O}(\tau)$ terms dropped, the connection matrix is found to be

$$\mathbf{F}(\infty, -\infty) = \begin{pmatrix} e^{2K_{21} - iK_{32}}\left[\sqrt{1+e^{-2K_{21}}} - e^{2iK_{32}}\right] & ie^{iK_{32}}\left[\sqrt{1+e^{-2K_{21}}} - e^{-2iK_{32}}\right] \\ \text{ind.} & \text{ind.} \end{pmatrix} \tag{3.6.13}$$

The QNM generating equations are found by requiring the appropriate part of this matrix to be zero. Namely,

$$\boxed{\Re\{\Omega\} \lessgtr 0 \quad \Rightarrow \quad \sqrt{1+e^{-2K_{21}}} = e^{\mp K_{32}}} \tag{3.6.14}$$

CHAPTER 4

Monodromy Method

4.1 Monodromy Technique

In studying the problem of quasi-normal modes, we see that it essentially reduces to finding a solution to Schröndiger type differential equation. We are interested in the solution for the "physical" region $r_+ < r < \infty$ i.e. outside the black hole.

This approach to solving our problem starts by extending the domain of the problem to the complex r-plane. By general theory of differential equations, any solution in the physical region will naturally extend into the whole complex plane.

The coordinate singularity of the metric at the horizon also shows up in the equation itself. As a result, the solution will be multivalued there, i.e. will naturally extend to multiple Riemann sheets. It is the monodromy of an equation that encodes how its solutions vary from one Riemann sheet to the next.

We are going to calculate the monodromies of the two solutions that correspond to our boundary conditions. Then, we will look for those (quasi) frequencies ω that make the monodromies equal. Essentially, we calculate the "eigenvalues ω" of our problem by imposing the boundary conditions.

Every monodromy corresponds to a closed contour in the complex plane which, in order to be non-trivial, should enclose a singularity (in this case, the one at $r = r_+$). We, thus, have to find two *essentially* different contours where each one encodes a different boundary condition.

The first contour is an infinitesimal circle around the singularity at $r = r_+$. By taking the appropriate limits in the differential equation, we match its solutions with the boundary condition at the horizon. The monodromy can be then straightforwardly calculated by computing the residue there.

The second contour is a bit more tricky. Starting by the solution for $r \to \infty$, we analytically extend it to negative imaginary infinity, $-i\infty$. From there, we calculate and follow anti-Stokes

lines crossing the real r axis "behind" the horizon, i.e. at some $r < r_+$ and continue to $+i\infty$. Finally, the solution is analytically extended back to where we started from, spatial infinity.

It has to be noted that this method yields results valid only in the highly damped limit $\Im(\omega) \to \infty$. This is advantageous since this regime is not easily accessible by other methods. At the same time however, it leaves out less damped modes which are more experimentally relevant.

4.2 Monodromy: an example

In order to make it clearer to the reader what the monodromy of a differential equation is and how it works, we shall give an example by studying the differential equation

$$\frac{d^2\psi}{dz^2} + \frac{\psi}{4z^2} = 0 \tag{4.2.1}$$

The general solution to this differential equation can be shown to be

$$\psi(z) = \mathbf{c} \cdot \mathbf{f}(z), \quad \mathbf{f}(z) = \begin{pmatrix} \sqrt{z} & \sqrt{z}\ln z \end{pmatrix} \tag{4.2.2}$$

where $\mathbf{c}$ is a constant vector.

It is evident from the differential equation that there is a singularity at $z = 0$. This reflects on the solutions being multivalued around that point. The monodromy of this equation will tell us how a specific solution ψ changes from one Riemann sheet to the next (i.e. when going around the singularity). Let us investigate each of the f_i's separately. Let $z = re^{i\theta}$ and then let z perform a clockwise rotation around $z = 0$ by allowing $\theta \to \theta + 2\pi$. Start from $f_1(z) = \sqrt{z}$.

$$\sqrt{z} = \sqrt{r}\exp\left(\frac{i\theta}{2}\right) \to e^{i\pi}\sqrt{r}\exp\left(\frac{i\theta}{2}\right) = -\sqrt{z}$$
$$f_1(z) \to -f_1(z) \tag{4.2.3}$$

This, of course, was expected. It is known that performing a clockwise rotation around 0 gives the opposite sign of the square root. Let us do the same for $f_2(z) = \sqrt{z}\ln z$.

$$\sqrt{z}\ln z = \sqrt{r}\exp\left(\frac{i\theta}{2}\right)(\ln r + i\theta) \to e^{i\pi}\sqrt{r}\exp\left(\frac{i\theta}{2}\right)(\ln r + i\theta + 2\pi i) = -\sqrt{z}\ln z - 2\pi i\sqrt{z}$$
$$f_2(z) \to -f_2(z) - 2\pi i f_1(z) \tag{4.2.4}$$

Here, we see an example of the Stokes phenomenon. By analytically continuing one solution (f_2) to another region of the complex plane (in this case, a different Riemann sheet), we have "switched on" the other solution (f_1).

The monodromy matrix $\mathbf{\Phi}$ is defined so that

$$\theta \to \theta + 2\pi \quad \Rightarrow \quad \mathbf{f}(z) \to \mathbf{\Phi} \cdot \mathbf{f}(z) \tag{4.2.5}$$

It can be derived by putting (4.2.3) and (4.2.4) together from which we get that

$$\mathbf{\Phi} = -\begin{pmatrix} 1 & 0 \\ 2\pi i & 1 \end{pmatrix} \tag{4.2.6}$$

4.3 Quasi-normal modes and the monodromy method

Following the work done in [26] we introduce the ansatz $u = \sqrt{\Delta}R$ in (1.3.16) which reduces to the Schrödinger like equation

$$\frac{d^2u}{dr^2} + Q^2(r)u = 0 \tag{4.3.1}$$

$$Q^2(r) = \frac{\tilde{Q}_2(r)\omega^2 + \tilde{Q}_1(r)\omega + \tilde{Q}_0(r) - \lambda_{ml}\Delta}{\Delta^2} \tag{4.3.2}$$

where

$$\tilde{Q}_2(r) = \left(r^2 + a^2\right)^2 - a^2\Delta \tag{4.3.3a}$$

$$\tilde{Q}_1(r) = -4Mram \tag{4.3.3b}$$

$$\begin{aligned}\tilde{Q}_0(r) &= a^2m^2 - \mu^2r^2\Delta + \frac{1}{4}\left(\left(\Delta'\right)^2 - 2\Delta\Delta''\right) \\ &= a^2m^2 - \mu^2r^2\Delta + M^2 - a^2\end{aligned} \tag{4.3.3c}$$

Remember from §1.3.3 that $\lambda_{ml} = \lambda_{ml}(-ic)$ is a non-trivial function of the parameter c given by $c^2 = a^2\left(\omega^2 - \mu^2\right)$. We want to incorporate this dependence in the $\tilde{Q}_i$ functions.

In order for this method to work, we study the highly damped region $\Im\omega \to \infty$. In this limit, note that $c^2 \to -\infty$ so that $c \to i\infty$. As a result, the valid expansion for λ_{ml} is that given by (A.4.1) which we expand with respect to ω

$$\lambda_{ml} = -iap\omega + \left(m^2 - \frac{p^2+5}{8}\right) + O\left(\frac{1}{\omega}\right) \quad \text{with} \quad p = 2(l-m)+1 \tag{4.3.4}$$

Again, it is important to note that this expansion is valid *only* for $|\Im\omega| \to \infty$. With this at hand, we can now rewrite (4.3.2) as

$$Q^2 = \frac{Q_2\omega^2 + Q_1\omega + Q_0 + O\left(\omega^{-1}\right)}{\Delta^2} \tag{4.3.5}$$

where the Q_i's now include the contributions from λ_{ml} and are given by

$$Q_2(r) = \tilde{Q}_2(r) \tag{4.3.6a}$$

$$Q_1(r) = \tilde{Q}_1(r) + i\Delta\lambda_1\,, \;\; \lambda_1 = -a\left[2(l-m)+1\right] \tag{4.3.6b}$$

$$Q_0(r) = \tilde{Q}_0(r) + \Delta\lambda_0\,, \;\; \lambda_0 = m^2 - \frac{\left[2(l-m)+1\right]^2 - 5}{8} \tag{4.3.6c}$$

It is much more convenient, though, for one to work with potentials of the form $Q^2 = \omega^2 - V$ such that $V = O\left(\omega^0\right)$. Bearing in mind that we are working in the limit $\omega \to \infty$, we can achieve this by defining a non-conventional tortoise coordinate z such that

$$z = \int_{r_0}^{r} q(r')dr'\,, \;\; q(r) = \frac{\sqrt{Q_2 + Q_1\omega^{-1}}}{\Delta} \tag{4.3.7}$$

and using a new "radial" function $\hat{R} = \sqrt{q}u$. In using these expressions, care must be taken as to the integrating contour since $q(r)$ has singularities at $r = r_{\pm}$. By these transformations, the original equation (4.3.1) becomes

$$\frac{d^2\hat{R}}{dz^2} + \left[\omega^2 - V + \mathrm{O}\left(\frac{1}{\omega}\right)\right]\hat{R} = 0 \tag{4.3.8}$$

where $V = \mathrm{O}\left(\omega^0\right)$:

$$V = \frac{\left(Q_2 Q_2'\right)\left(\Delta\Delta'\right) + \left(Q_2\Delta'\right)^2 + Q_2 Q_2''\Delta^2}{4Q_2^3} - \frac{16Q_0Q_2^2 + 5\Delta^2\left(Q_2'\right)^2 + 8Q_2^2\Delta\Delta''}{16Q_2^3} \tag{4.3.9}$$

Let us note that in these coordinates, the potential has the following behavior:

$$V(r_+) = \frac{m^2\left(2Mr_- - a^2\right)}{4a^2M^2} \tag{4.3.10}$$

$$V(r \to \infty) = \mu^2 \tag{4.3.11}$$

4.3.1 Monodromy Φ_1

With these at hand, let us investigate the solution at the horizon. In the limit of $\omega \to \infty$ the boundary condition becomes $\hat{R}(r \to r_+) \sim \exp\left(-i\Omega z\right)$ with Ω in the case being

$$\begin{aligned}\Omega_1 &= \sqrt{\omega^2 - V(r_+)} = \omega\sqrt{1 - \frac{m^2\left(2Mr_- - a^2\right)}{4a^2M^2\omega^2}} \\ &= \omega + \mathrm{O}\left(\frac{1}{\omega^2}\right)\end{aligned} \tag{4.3.12}$$

Expanding $q(r)$ from (4.3.7) in a Laurent series around $r = r_+$ we get

$$q(r) = \frac{\sigma_+}{r - r_+} + \sum_{n=0}^{\infty} q_n\left(r - r_+\right)^n \tag{4.3.13}$$

where σ_+ is the residue of $q(r)$ at $r = r_+$.

Consequently, $z(r)$ can be written as

$$z(r) = \sigma_+ \ln\left(r - r_+\right) + \sum_{n=0}^{\infty} \frac{q_n}{n+1}\left(r - r_+\right)^{n+1} \tag{4.3.14}$$

so that close to the horizon, $r \to r_+$, the behaviour of $z(r)$ is logarithmic $z(r) = \sigma_+ \ln\left(r - r_+\right)$. As such, the boundary condition now reads

$$\hat{R}(r \to r_+) \sim \left(r - r_+\right)^{-i\Omega_1\sigma_+} \tag{4.3.15}$$

As it can be seen, the solution $\hat{R}$ is multivalued around the horizon. It is exactly this multivaluedness that we shall exploit with this method.

We thus define the monodromy Φ_1 as the multiplicative factor of the solution when one performs a clockwise rotation around r_+ on a circle of radius $\epsilon \to 0$. Calculating σ_+ we find that

$$\Omega_1 \sigma_+ = \frac{r_+^2 + a^2}{r_+ - r_-}\omega - \frac{am}{r_+ - r_-} + \mathrm{O}\left(\frac{1}{\omega}\right) \tag{4.3.16}$$

By virtue of (4.3.15), Φ_1 is given by

$$\boxed{\Phi_1 = \exp\left(-2\pi\Omega_1\sigma_+\right)} \tag{4.3.17}$$

4.3.2 Monodromy Φ_2

We now proceed with the calculation of the second monodromy, Φ_2. We shall take advantage of the fact that the WKB approximation gives easy-to-compute results when one is working along a Stokes line.

Let us start by investigating the structure of $z(r)$ in the complex plane. Denote by t_i the turning points of $q(r)$, as given in (4.3.7), i.e. $q(t_i) = 0$. In the limit of large frequencies $(\omega \to \infty)$ these coincide with the roots of $Q_2(r)$ so that $t_i = r_i + O\left(\omega^{-1}\right)$.

The r_i's are given by $Q_2(r) = r\left(r^3 + a^2 r + 2Ma^2\right)$ with roots $\{0, r_0, r_{12}\}$. Although we shall not need them explicitly, their analytic formulas are

$$r_0 = \frac{\sqrt[3]{3}\left(a^2\left(\sqrt{3}\sqrt{a^2+27M^2} - 9M\right)\right)^{2/3} - 3^{2/3}a^2}{3\sqrt[3]{a^2\left(\sqrt{3}\sqrt{a^2+27M^2} - 9M\right)}} \tag{4.3.18a}$$

$$r_{12} = \frac{\pm i\sqrt[3]{3}\left(\sqrt{3} \pm i\right)\left(a^2\left(\sqrt{3}\sqrt{a^2+27M^2} - 9M\right)\right)^{2/3} + \sqrt[6]{3}\left(\sqrt{3} \pm 3i\right)a^2}{6\sqrt[3]{a^2\left(\sqrt{3}\sqrt{a^2+27M^2} - 9M\right)}} \tag{4.3.18b}$$

For $a = 0$, $Q_2(r) = r^4$ so that all roots coincide and are equal to zero. Otherwise, r_0 is always real and negative, while r_{12} are complex conjugate with an always positive real part.

The turning points of $q(r)$ are of importance because it is from there that Stokes and anti-Stokes lines emanate. They are given by $\Im(i\omega z) = 0$ and $\Re(i\omega z) = 0$ respectively. In the limit $\Im\omega \to \infty$ we have that $\Re\left(i\omega z\right) = 0$ is equivalent to $\Re z = 0$. We have to remember that those lines are always defined with respect to the point from which they emanate (see §3.5.1).

Let is investigate the behavior of $q(r)$ around the turning points $r = t_i$ and the singular points

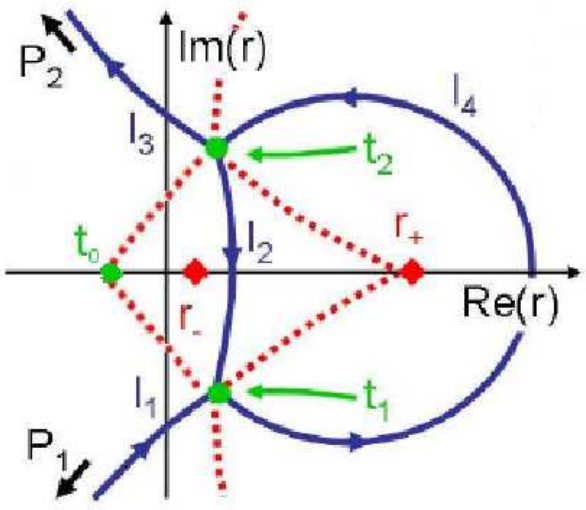

Figure 4.1: Illustration of anti-Stokes(solid) and Stokes (dashed) lines emanating from the turning points t_i's (disks) in the complex r-plane in the highly-damped limit. The inner and outer horizon radii $r_\pm$ (diamonds) and components of the contour are also shown. Arrows along anti-Stokes lines denote the direction of increasing $\Im(i\omega z)$. [26]

$r = r_\pm, \infty$. Respectively,

$$q(r) = \sum_{n=0}^{\infty} c_n^i \, (r - t_i)^{n+1/2} \tag{4.3.19a}$$

$$q(r) = \pm \frac{A + O\left(\omega^{-1}\right)}{r - r_\pm} + \sum_{n=0}^{\infty} c_n^\pm \, (r - r_\pm)^n \ , \quad A > 0 \tag{4.3.19b}$$

$$q(r) = 1 + \sum_{n=1}^{\infty} \frac{c_n^\infty}{r^n} \tag{4.3.19c}$$

For z, these mean that

$$(z - z_i) \sim (r - t_i)^{3/2} \tag{4.3.20a}$$

$$(z - z_\pm) \sim \pm \ln (r - r_\pm) \tag{4.3.20b}$$

$$(z - z_\infty) \sim r \tag{4.3.20c}$$

From the equations around $r = t_i$, we can tell that there are three Stokes lines and three anti-Stokes lines emanating from each of the two turning points. Two anti-Stokes lines connect t_1 to t_2; one crossing the real line on (r_-, r_+) and the other on (r_+, ∞). The rest of them extend to P_i with $|P_i| \to \infty$ and $\arg P_i = \pm\pi/2$. As for the Stokes lines, they emanate between every two anti-Stokes lines. Again, two of them connect t_1 to t_2, one via r_+ and the other through t_0 (see Fig.4.1).

Let us define the following contours. Begin with the anti-Stokes lines along the segments $[l_1 : P_1 \to t_1]$, $[l_2 : t_1 \to t_2]$ via (r_-, r_+) and $[l_3 : t_2 \to P_2]$. Let $[l_\infty : P_1 \to P_2]$ be along a semi-

circle with $|R| \to \infty$ and $-\pi/2 < \arg R < \pi/2$. We now define Φ_2 to be the monodromy along the contour $C_2 = \{l_1, l_2, l_3, l_\infty\}$. We shall cut the complex plane along l_2.

We start with the solution at spatial infinity given by

$$\hat{R}(r \to \infty) = \exp(i\Omega_2 z) \quad \text{where} \quad \Omega_2 = \sqrt{\omega^2 - V(\infty)} \xrightarrow[\omega\to\infty]{} \omega + \mathrm{O}\left(\frac{1}{\omega^2}\right) \tag{4.3.21}$$

In terms of the vector $\mathbf{a}$, this is also given by $\mathbf{a}(\infty) = (a_+,\ 0)$. We choose to express this solution with respect to t_1, the lower limit of the z integral for reasons that will become apparent shortly. Any other choice will differ only within a multiplicative phase factor.

For $\Re(\Omega_2) < 0$, this solution can be analytically continued to P_1 [26] and it is still $\mathbf{a}(P_1) = (a_+,\ 0)$. Remember that along an anti-Stokes lines, the connection matrix $\mathbf{F}$ is approximately equal to the unit matrix (see §3.5.3 and [23]). We propagate the solution from l_1 to l_2 using the connection matrices $\mathbf{F}(z_6, z_4)\mathbf{F}(z_4, z_2)$ from (3.5.3). It is evident that

$$\mathbf{F}(l_2,\ l_1) \simeq \begin{pmatrix} 0 & i \\ i & 1 \end{pmatrix} \tag{4.3.22}$$

As done for the three turning points problem of §3.6.5, in order to apply the connection matrix for propagating our solution from l_2 to l_3, we first have to express it with respect to t_2 rather than t_1 effectively introducing a phase shift

$$\mathbf{\Phi}(t_2,\ t_1) = \mathrm{diag}\left[\exp(+i\Omega_2\phi),\ \exp(-i\Omega_2\phi)\right] \quad \text{where} \quad \phi = \int_{l_2} q(r)dr \tag{4.3.23}$$

Moving on, the connection matrix from l_2 to l_3 is now given by $\mathbf{F}(z_4, z_2)\mathbf{F}(z_2, z_0)$ of (3.5.3).

$$\mathbf{F}(l_3,\ l_2) \simeq \begin{pmatrix} 1 & i \\ i & 0 \end{pmatrix} \tag{4.3.24}$$

Continuing from P_2 back to P_1 but, this time, along l_∞ leaves the solution approximately invariant, i.e. $\mathbf{F}(P_2,\ P_1;\ l_\infty) \simeq \mathbb{I}_2$[1]. What is more, in order to consistently close the contour, we have to re-express the solution with respect to t_1, i.e. insert an extra phase matrix $\mathbf{\Phi}(t_1,\ t_2) = [\mathbf{\Phi}(t_2,\ t_1)]^{-1}$. As a result,

$$\mathbf{F}(C_2) = \mathbf{\Phi}(t_1,\ t_2)\cdot\mathbf{F}(l_3,\ l_2)\cdot\mathbf{\Phi}(t_2,\ t_1)\cdot\mathbf{F}(l_2,\ l_1) = \begin{pmatrix} -e^{-2i\Omega_2\phi} & i\left(1 + e^{-2i\Omega_2\phi}\right) \\ 0 & -e^{2i\Omega_2\phi} \end{pmatrix} \tag{4.3.25}$$

By definition, $\mathbf{\Phi}_+ \cdot \mathbf{F}(C_2) \cdot \mathbf{a}(\infty) = \Phi_2\mathbf{a}(\infty)$ where $\mathbf{\Phi}_+$ is an extra phase factor introduced by the enclosure of the singularity at $r = r_+$ and Φ_2 is the monodromy we are looking for. Consequently,

$$\Phi_2 = -\exp\left(2\pi\Omega_1\sigma_+ - 2i\Omega_2\int_{l_2} q(r)dr\right) \tag{4.3.26}$$

[1] in actuality, this is true only for the dominant part of the solution

4.3.3 The QNM generating equation

Requiring that the two monodromies Φ_1 and Φ_2 are equal, we can constrain the frequencies ω to a discrete set of values. These values constitute the set of *quasi-normal modes* of our problem.

$$\Phi_1 = \Phi_2 \quad \Rightarrow \quad 2\pi\Omega_1\sigma_+ - i\Omega_2 \int_{l_2} q(r)dr = i\pi\left(n + \frac{1}{2}\right) \tag{4.3.27}$$

We now expand the equation above in the limit of large frequencies. $\Omega_1\sigma_+$ has already been studied in (4.3.16) which we rewrite for clarity and completeness.

$$\Omega_1\sigma_+ = \frac{r_+^2 + a^2}{r_+ - r_-}\omega - \frac{am}{r_+ - r_-} + \mathrm{O}\left(\frac{1}{\omega}\right) \tag{4.3.28a}$$

$$\Omega_2 \int_{l_2} q(r)dr = \omega \int_{l_2} \frac{\sqrt{Q_2}}{\Delta}dr + \int_{l_2} \frac{\tilde{Q}_1}{2\sqrt{Q_2}\Delta}dr + i\int_{l_2} \frac{\lambda_1}{2\sqrt{Q_2}}dr + \mathrm{O}\left(\frac{1}{\omega}\right) \tag{4.3.28b}$$

Remember that the l_2 contour connects two points in the complex plane which are complex conjugates, $t_1 = t_2^*$. Since all integrand functions have real coefficients, we have as a result that all integrals at the right-hand side of (4.3.28b) are purely imaginary. Let

$$\delta_2 = -i\int_{l_2} \frac{\sqrt{\tilde{Q}_2}}{\Delta}dr\,, \quad m\delta_1 = -i\int_{l_2} \frac{\tilde{Q}_1}{2\sqrt{\tilde{Q}_2}\Delta}dr \quad \text{and} \quad \delta_0 = i\int_{l_2} \frac{\lambda_1}{2\sqrt{\tilde{Q}_2}}dr \tag{4.3.29}$$

such that all δ_i's are real. Their analytic expressions can be expressed in terms of elliptic integrals. However, these formulas are quite extensive and will not be presented here (see [27]). The QNM equation now reads

$$\omega\left(\delta_2 + \frac{2\pi(r_+^2 + a^2)}{r_+ - r_-}\right) + \left(m\delta_1 - \frac{2\pi am}{r_+ - r_-}\right) = i\left\{\pi\left(n + \frac{1}{2}\right) + \delta_0\right\} \tag{4.3.30}$$

Separating the real from the imaginary part is now straightforward and will yield the highly damped equation for QNMs

$$\Re\{\omega\} = \frac{2\pi am - (r_+ - r_-)m\delta_1}{(r_+ - r_-)\delta_2 + 2\pi(r_+^2 + a^2)} \quad \text{and} \quad \Im\{\omega\} = \frac{[\pi(2n+1) + 2\delta_0](r_+ - r_-)}{2(r_+ - r_-)\delta_2 + 4\pi(r_+^2 + a^2)} \tag{4.3.31}$$

However, setting

$$\tilde{\delta}_2 = (r_+ - r_-)\,\delta_2 + 2\pi\left(r_+^2 + M^2J^2\right) \tag{4.3.32}$$

$$\tilde{\delta}_1 = 2\pi a - (r_+ - r_-)\,\delta_1 \quad \text{and} \quad \tilde{\delta}_0 = -2a\,(r_+ - r_-)\,\frac{\delta_0}{\lambda_1} \tag{4.3.33}$$

we can decouple the parameter dependencies and have that

$$\omega = mf_0 + i\Big\{f_1 + nf_2 + (l-m)f_3\Big\} \tag{4.3.34}$$

$$f_0 = \frac{\tilde{\delta}_1}{\tilde{\delta}_2}, \quad f_1 = \frac{\tilde{\delta}_0 + \pi\,(r_+ - r_-)}{2\tilde{\delta}_2}, \quad f_2 = \frac{\pi\,(r_+ - r_-)}{\tilde{\delta}_2}, \quad f_3 = \frac{\tilde{\delta}_0}{\tilde{\delta}_2}, \tag{4.3.35}$$

where the f_i's are functions of the black hole's angular momentum a and mass M *only*. Note that the dependence on the scalar mass has (long) dropped out of the calculation. This is a property of the highly damped limit.

CHAPTER 5

QNM Numerics & Computation

5.1 Numerical Solutions

In the sections §3.6 and §4.3 we derived the QNM generating equation with two different methodologies. In order to perform numerical calculations, we rescale the quantities involved so that they are dimensionless. Specifically,

$$r = My, \quad a = Mj, \quad \omega \to \frac{\omega}{M}, \quad \mu \to \frac{\mu}{M}, \quad f_i \to \frac{f_i}{M} \tag{5.1.1}$$

5.2 Matrix WKB

The first one is based on the matrix WKB approximation. The form of the equation depends on the number of turning points of the potential Q^2 which we label by x_i, ordered so that $x_i < x_{i+1}$. The potential is given by (3.6.3) and for our purposes is

$$Q(z) = \sqrt{a(z)\omega^2 + b(z)\omega + c(z) + d(z)\lambda(\omega)}, \quad \lambda(\omega) = \lambda_{ml}\left(-ij\sqrt{\omega^2 - \mu^2}\right) \tag{5.2.1}$$

$$d(z) = -\frac{\Delta}{\left(r^2+a^2\right)^2}, \quad a(z) = 1 - \frac{a^2\Delta}{\left(r^2+a^2\right)^2}, \quad b(z) = -\frac{4Mram}{\left(r^2+a^2\right)^2}$$

$$c(z) = -\frac{\Delta\mu^2}{r^2+a^2} + \frac{a^2\left(\Delta\mu^2+m^2\right)}{\left(r^2+a^2\right)^2} - \frac{\left(3r^2-4Mr+a^2\right)\Delta}{\left(r^2+a^2\right)^3} + \frac{3r^2\Delta^2}{\left(r^2+a^2\right)^4}$$

Let

$$K_{ij} = \int_{x_i}^{x_j} |Q(z)|\, dz = c_{ij} \sum_{n=0}^{\infty} \omega^n \int_{x_i}^{x_j} \hat{Q}_n(z) dz, \quad c_{ij} \in \{\pm 1, \pm i\} \tag{5.2.2}$$

where $\hat{Q}_n$ are the Taylor expansion coefficients of $Q(z)$ around $\omega = 0$. We can deduce from the complex phases in (3.6.9) that $c_{12} = i$ and $c_{23} = 1$. We calculate the $\hat{Q}_n$'s as follows

$$\hat{Q}_0 = \sqrt{j\mu\left(djl_2\mu - 1\right) + dl_0}$$

$$\hat{Q}_1 = \frac{b}{2\sqrt{j\mu\left(djl_2\mu - 1\right) + dl_0}}$$

$$\hat{Q}_2 = \frac{\mu\left(2dj^2l_2\mu\left(2a\mu - 2dj^2l_2\mu + 3j\right) - 2j(2a\mu + j) - b^2\right) + 2dl_0\left(2a\mu - 2dj^2l_2\mu + j\right)}{8\mu\left(j\mu\left(djl_2\mu - 1\right) + dl_0\right)^{3/2}}$$

$$\hat{Q}_3 = \frac{b\left(\mu\left(2dj^2l_2\mu\left(-2a\mu + 2dj^2l_2\mu - 3j\right) + 2j(2a\mu + j) + b^2\right) + 2dl_0\left(-2a\mu + 2dj^2l_2\mu - j\right)\right)}{16\mu\left(j\mu\left(djl_2\mu - 1\right) + dl_0\right)^{5/2}}$$

The l_i's are the power series expansion coefficients of λ_{ml} and are given in (A.3.2). We shall perform our calculations up to second order in ω and use the third order term to evaluate our error (remember that $l_3 = 0$).

For $\Omega = \omega - \frac{mr_-}{2aM}$, we explored the following two cases

1. Two turning points: $\quad \Re\{\Omega\} < 0, \quad K_{12} = -i\pi\left(n + \frac{1}{2}\right)$
2. Three turning points: $\quad \Re\{\Omega\} \lesseqgtr 0, \quad \sqrt{1 + \exp\left(-2K_{21}\right)} = \exp\left(\mp K_{32}\right)$

As a result, for each parameter set $\{j,\ \mu,\ m,\ l\}$ (M drops out), we shall first have to determine the number and position of the turning points x_i. Then, we numerically evaluate the integrals of $\hat{Q}_n$ and solve the appropriate equation (either algebraic or transcendental).

5.2.1 Computing the error τ

Before we proceed with the calculation of the quasi-normal frequencies, we first compute the error measure τ. As indicated in §3.4 and §3.5, in order for the estimates used to be accurate, $\tau \ll 1$. While its calculation requires knowledge of ω after all, numerical evaluation of τ for random values of ω gives an extremely large error value $\ln(\tau) \sim \mathrm{O}\left(10^1\right)$.

Trying to take advantage of this fact, we search for values of ω for which the error is small enough for our estimates to be valid. However, we come up with no results. Trying values in a discretized grid in the complex ω-plane never gives an error even remotely close to 1 (which would still be not good enough but could indicate being close to a potential quasi-normal frequency).

5.2.2 Computing the roots of Q^2

What is more, another complication arises in the computation of the roots of the potential Q. In order to calculate them we bring it into the rational form $Q^2(r) = q(r)/p(r)$ where q, p are polynomials in r. Unfortunately, $q(r)$ is 8^{th} order in r which make the search of its roots (and in extension Q's) possible only through numerical means.

However, both q and Q are functions of the frequency, along with the rest of the problem's parameters. As a result, in order to find the roots, one has to know the quasi-normal frequency ω and vice-versa.

Nevertheless, this does not have to be the end of this story. An iterative scheme can be devised where one "shoots" a value for ω, calculates the roots of Q, revises the guess on the frequency and starts all over again until the algorithm converges.

Numerical simulations for various values of the parameters show that, in most cases, the potential has *no* roots in the area outside the event horizon. This property makes an iterative scheme difficult to implement as well as probably not convergent. Of course, *more research on this subject is required in order to come to a more solid conclusion regarding this matter.* However, such research belongs mainly to the field of computational physics and numerical analysis which is outside of the scope of this thesis and would require more time.

5.3 Monodromy

The second method is based on the monodromy of the solution in the complexified r plane around the horizon at r_+. It is valid only in the highly damped limit, i.e. $\Im\{\omega\} \gg 0$. The QNM frequencies are given by (4.3.31) and their computation amounts to calculating the δ_i's. However, due to the number of different parameters, it is much more convenient to calculate the f_i's (4.3.35) since they depend only on the angular momentum j. Their numerical computation was done in Mathematica and the source code can be found in App. C.1. Remember that

$$\omega = m f_0 + i\Big\{ f_1 + n f_2 + (l-m) f_3 \Big\} \tag{5.3.1}$$

Figure 5.2 presents plots of the f_i's. Fitting the numerical data to power series over j, we get [1] [2]

$$f_0^{(\text{fit})} = -0.151\, j^{1/3} + 0.1482\, j - 0.0690\, j^2 + 0.0211\, j^3 \tag{5.3.2a}$$

$$f_1^{(\text{fit})} - 1/8 = 0.07618\, j^{1/3} + 0.0090\, j - 0.0051\, j^2 + 0.00044\, j^3 \tag{5.3.2b}$$

$$f_2^{(\text{fit})} - 1/4 = 0.01100\, j - 0.0045\, j^2 - 0.0003\, j^3 \tag{5.3.2c}$$

$$f_3^{(\text{fit})} = 0.15299\, j^{1/3} + 0.00446\, j - 0.0016\, j^2 - 0.0012\, j^3 \tag{5.3.2d}$$

In Fig.5.3 the relative deviations $\rho_i = \frac{f_i^{(\text{fit})} - f_i}{f_i}$ of the fits from the numerical data are plotted. The maximum value of ρ occurs for f_0 and is of the order of 0.4%.

Remember that these QNMs are valid only when $\Im\{\omega\} \to \infty$ or equivalently $\omega_I \gg 1$. Note that the functions in the imaginary part of ω are positive and monotonically increasing as

[1] The fits were done in **Mathematica 7**™ using the **NonlinearModelFit** function. j was sampled in $[0, 0.95]$ with a spacing of $\Delta j = 0.01$.

[2] The constant terms in f_1 and f_2 are calculated analytically.

Figure 5.1: Zeeman-like splitting of $n = 100$, $l = 2$, $m = -2...2$ (from right to left) modes as j ranges in $[0, 1)$.

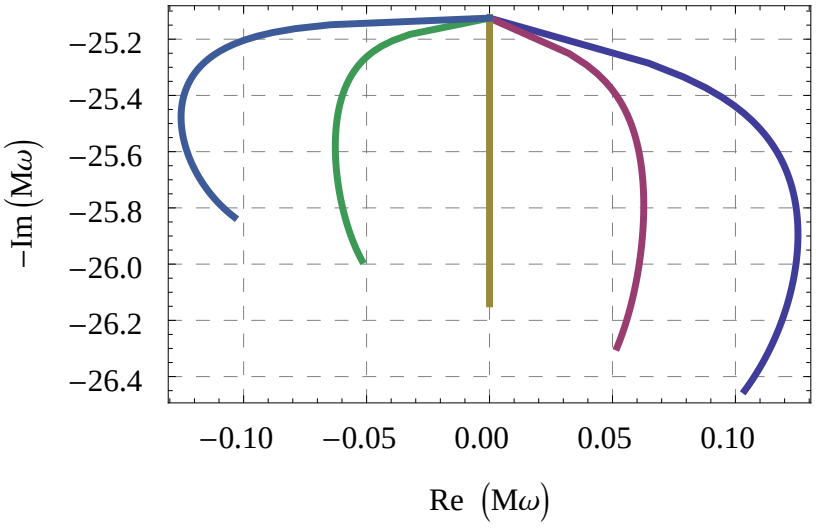

Figure 5.2: Plots of f_i's as functions of j

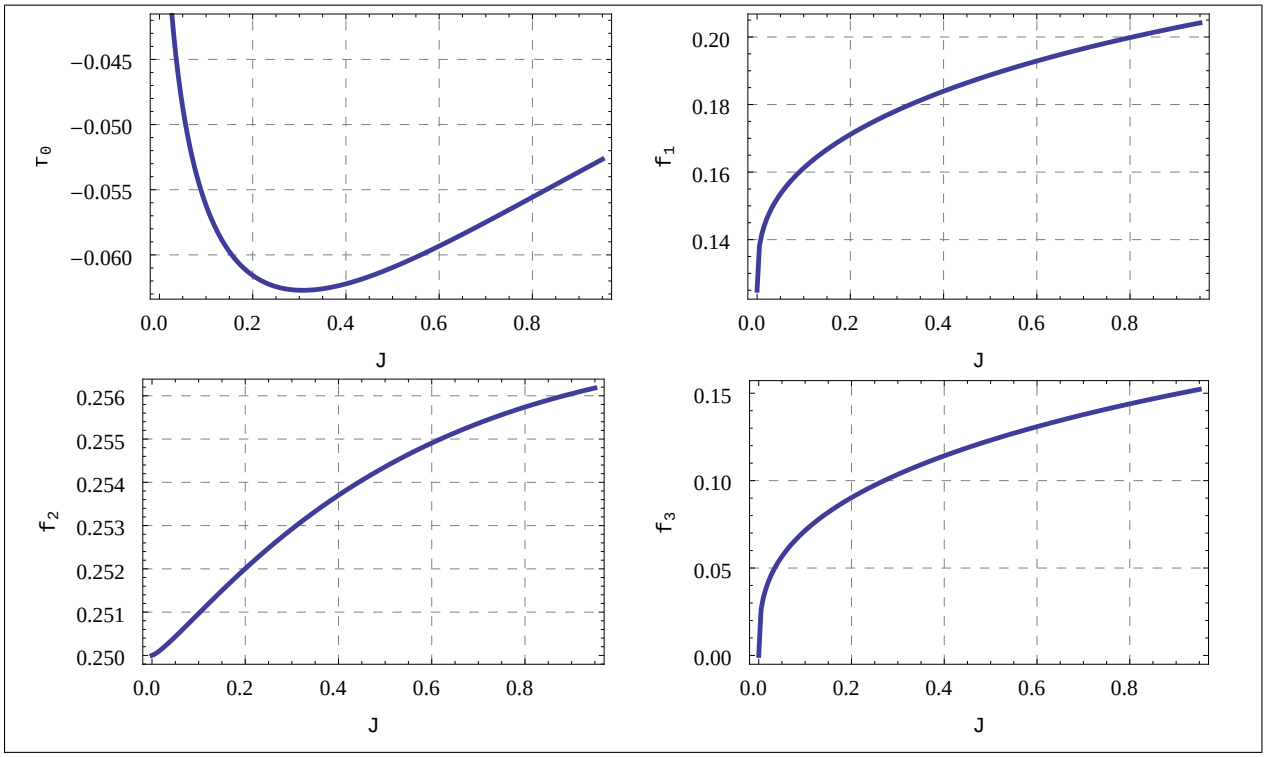

Figure 5.3: Plots of $\rho_i = \frac{f_i^{(\mathrm{fit})} - f_i}{f_i}$ as functions of j scaled by a factor of 10^2

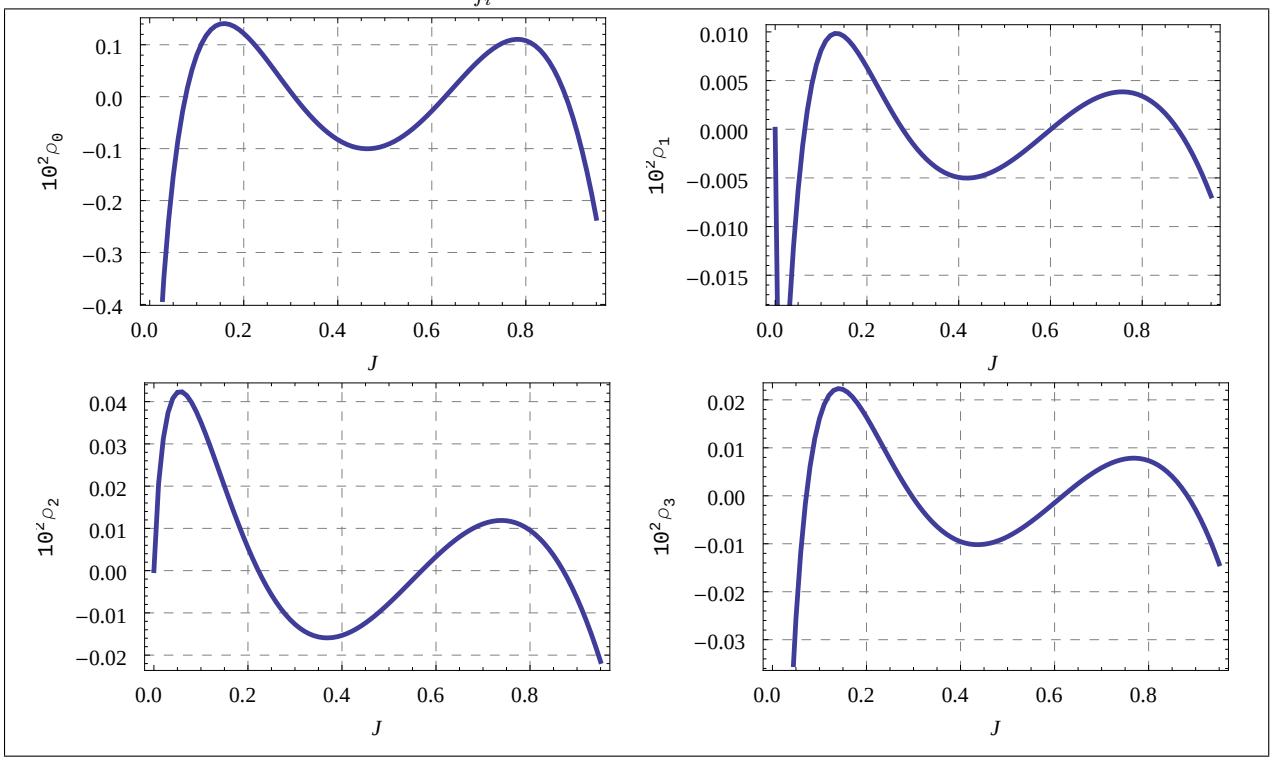

functions of j. It is not difficult to see that every mode takes its minimum value as $m \to l$ and $j \to 0$ so that $\omega_I \geq \frac{1}{8} + \frac{n}{4}$. As a result, the corrections will be of the order

$$\frac{1}{\omega_I} \leq \frac{8}{2n+1} \tag{5.3.3}$$

and, thus as expected, the approximation stands for modes with $n \gg 1$.

The power fits (5.3.2) and plots of fig. 5.2 are in agreement with the original paper [26] as well as with the results given in review [1] and references therein. Care must taken, however, when one compares results as plotted/fitted quantities differ within factors of 2 or 1/2 between different publications.

CHAPTER 6

Conclusions

In this work, we have studied two different methods for the calculation of scalar quasi-normal modes in Kerr background. We gave an introduction in black hole spacetimes. As an introductive toy model, we studied the BTZ black static BH and derived its exact scalar QNM. What is more, we considered both the Schwarzschild, zero angular momentum and charge, as well as the Kerr, rotating and uncharged, black holes.

Using the symmetries of these spacetimes, we provided an ansatz for the scalar field and performed separation of variables. The angular part of the equations were already considered solved in terms of *oblate spheroidal functions*. The only unsolved part of the equations is, thus, the radial part. However, we are only interested in the eigenvalues ω which correspond to the quasi-normal frequencies that we are looking for.

The main part of this thesis has thus been the study of two methods for the calculation of the quasi-normal frequencies, the matrix WKB approximation and the monodromy method.

6.1 Matrix WKB approximation

For the study of this method we followed the work done by Gal'tsov and Matiukhin in [25]. It is a generalization of the WKB approximation, also known as the method of matched assymptotic expansions.

The main advantage of this method is that it avoids the, sometimes, ambiguous asymptotic series used in the standard WKB approximation. Instead, the equation is transformed in such a way so that a convergent scheme can be devised. The problem is then reduced to a first-order *vector* differential equation which can be formally integrated.

This scheme looks for the eigenvalues ω that allow the two boundary conditions, at the horizon and at infinity, to be seamlessly "matched". Problems, however, arise due to the complicated dependence of the scalar potential on the eigenvalue ω.

We were unable to calculate the zeros of the scalar potential, quantities which are essential for the computation of the quasi-normal frequencies. Moreover, we did not manage to understand

how the estimates for the aforementioned quantities given in [25] are obtained. In contrast, our numerical simulations indicate that they are not always applicable.

Another problem we encountered is the large values of the error measure τ in our numerical simulations. The authors of [25] only comment on this error being small but do not refer to any numerical computations on it.

Last but not least, we have reservations about its theoretical validity as the formulas used require the effective potential to be real. Since, however, the potential Q is a function of the quasi-normal frequencies ω, this assumption seems to be invalid. The authors of [25] (as well as other papers that use this method) do not elaborate on this matter. The most widely accepted justification is that only at the end of the calculation the frequencies are analytically continued to complex values. This, however, we find inadequate.

Due to the aforementioned, even though the results given in [25] seem to agree with the literature, we are doubtful about the validity of the procedure used. As a result, even though this method is more generic when compared to the standard WKB approximation, its use for solving this problem requires additional research.

6.2 Monodromy method

For the study of this method we followed the work done by Keshet and Hod in [26]. This method takes advantage of the general analytic properties of differential equations in the complex plane.

The presence of a mathematical singularity at the event horizon makes the general solutions to the differential equation multi-valued there. This multi-valuedness, described by the monodromy of the equation, depends both on the quasi-normal frequencies ω as well as the boundary conditions. The monodromy around the horizon is calculated twice, once for each boundary condition. In order for the solutions to be consistent, i.e. both boundary conditions satisfied and thus the frequency ω indeed being a quasi-normal frequency, these two monodromies have to agree.

A characteristic of this method, which can be seen both as an advantage as well as a disadvantage, is that it is applicable only in the highly damped limit of $\Im\omega \to \infty$. Despite that, it is quite straightforward to apply and results which agree with the literature were readily obtained. It was shown that, in this limit, ω is indeed linear in both the angular numbers l and m as well as the harmonic number n.

More specifically, the real part of ω is proportional to m while its dependence on a/M is slightly more complicated and shown in Fig.5.2. The imaginary part of the frequency, while linear in n and $(l-m)$, turns out to be a monotonically increasing function of a/M as can be seen in the same figure.

6.3 Outlook

The authors regret that time limitations, circumstances as well as personal experience did not allow this thesis to be more extensive, complete and conclusive in its research view of *massive scalar QNMs*. However, as with all written works of this kind, a balance must be stricken between time and completeness and for better or worse this has been it. As a result, we would like to present the reader who has courageously reached this far with avenues of research that may be pursued as continuation of this work.

First and foremost, it has been evident through our work that the matrix WKB approximation has tremendous potential both for our problem as well as others. Nevertheless, we believe that there is still a lot of work to be done with it. More specifically and with respect to our problem,

1. Robust mathematical analysis on practically foregoing the requirement of the effective potential $Q(z)$ being real.
2. Analysis and investigation of an appropriate transformation (i.e. $q(z)$ function) so that the error τ remains small along the required path.
3. Derivation of next-order approximation of the connection formula.

Such matters are not adequately addressed in the literature and a robust analysis would as well provide good ground for other applications.

As far as the monodromy method is concerned, matters are quite more conclusively addressed. Still, since the method is applicable in the highly damped limit (i.e. $\Im\Omega \to \infty$), there is work to be done in deriving next order approximations.

Looking into the bigger picture, the next big step would be to apply the machinery developed to fields of higher spin (both bosonic and fermionic). What is more, it is of great importance for the AdS/CFT correspondence that this work is generalized to spacetimes with negative cosmological constant so that the results can readily be used in the dual theory. Even though some of these matters have in principle been addressed already, the authors feel that a comprehensive mathematical review would have much to offer in the field as it would shed light in subtle issues that are now hidden and/or understated (e.g. the complex valuedness of the effective potential Q).

Appendices

APPENDIX A

Spheroidal Functions

A.1 Spheroidal coordinates

A spheroid, or ellipsoid of revolution, is the surface obtained when one rotates an ellipse about one of its principal axes. In case this is the major axis, the result is called a *prolate* spheroid whereas in case the rotation is about its minor axis the result is an *oblate* spheroid.

The speroidal coordinates are related to cartesian coordinates by the transformation [28]

$$x = \frac{L}{2}\sqrt{(1-\eta^2)\,(\xi^2 \mp 1)}\cos\phi, y = \frac{L}{2}\sqrt{(1-\eta^2)\,(\xi^2 \mp 1)}\sin\phi, z = \frac{L}{2}\eta\xi \tag{A.1.1}$$

where the upper sign corresponds to prolate spheroidal coordinates while the lower sign to oblate.

In the prolate spheroidal system, the coordinates range in

$$-1 \leq \eta \leq 1\,, \quad 1 \leq \xi \leq \infty\,, \quad 0 \leq \phi \leq 2\pi \tag{A.1.2}$$

Surfaces of constant ξ define an ellipsoid of revolution whose major and minor axis are equal to $L\xi$ and $L\sqrt{\xi^2-1}$ respectively. The special case of $\xi = 1$ degenerates to a straight line along the z-axis on the segment $[-L/2, L/2]$. Surfaces of constant $|\eta|$ are hyperboloids of revolution of two sheets. Their generating line passes through the origin at an angle $\theta = \arccos\eta$ with respect to the z-axis while the degenerate surface $|\eta| = 1$ is the part of z-axis for which $|z| > L/2$. Finally, the ϕ coordinate is the same as in Cartesian coordinates so that surfaces of constant ϕ are planes through the z-axis at an angle of ϕ with respect to the x, z-plane.

In the oblate spheroidal system, the coordinates range in

$$-1 \leq \eta \leq 1\,, \quad 0 \leq \xi \leq \infty\,, \quad 0 \leq \phi \leq 2\pi \tag{A.1.3}$$

Surfaces of constant ξ are again ellipsoids of revolution whose major and minor axis this time are equal to $L\sqrt{\xi^2+1}$ and dL respectively. The special case $\xi = 0$ defines a disk of radius $L/2$ on the x, y-plane, centered at the origin. Surfaces of constant $|\eta|$ form a hyperboloid

of revolution of one sheet but with the same generating line as in prolate coordinates. This time, the case $|\eta| = 1$ *is* the z-axis while $\eta = 0$ is the x, y-plane except for the circular disk $\xi = 0$. The ϕ coordinate is the same as in the prolate system of coordinates mentioned in the previous paragraph.

Note that spheroidal coordinates are systems of orthogonal curvilinear coordinates, right-handed and cover all $\mathbb{E}^3$ space.

A.2 Spheroidal differential equations

Spheroidal functions come about as solutions of the scalar Helmholtz differential equation $\left(\nabla^2 + k^2\right)\psi = 0$ in spheroidal coordinates. After quite a bit of algebra, the differential equation obtained is

$$\left[\frac{\partial}{\partial\eta}\left(1-\eta^2\right)\frac{\partial}{\partial\eta} + \frac{\partial}{\partial\xi}\left(\xi^2 \mp 1\right)\frac{\partial}{\partial\xi} + \frac{\xi^2 \mp \eta^2}{\left(\xi^2 \mp 1\right)\left(1-\eta^2\right)}\frac{\partial^2}{\partial\phi^2} + c^2\left(\xi^2 \mp \eta^2\right)\right]\psi = 0 \tag{A.2.1}$$

with $c = \frac{kL}{2}$. It is important to note that one can switch the coordinate system of the differential equation from prolate to oblate by the transformations $\xi \to \pm i\xi,\ c \to \mp ic$.

Separations of variables is possible and the ansätze for equations (A.2.1) are

$$\psi_{mn} = \exp\left(im\phi\right)\begin{matrix} S_{mn}(c,\eta) & R_{mn}(c,\xi) \\ S_{mn}(-ic,\eta) & R_{mn}(-ic,-i\xi) \end{matrix} \tag{A.2.2}$$

R_{mn} is usually denoted as the "radial" part while S_{mn} is the angular solution. These functions satisfy the differential equations

$$\left\{\frac{d}{d\eta}\left[\left(1-\eta^2\right)\frac{d}{d\eta}\right] + \left[\lambda_{mn} \mp c^2\eta^2 - \frac{m^2}{1-\eta^2}\right]\right\}\begin{matrix} S_{mn}(c,\eta) \\ S_{mn}(-ic,\eta) \end{matrix} = 0 \tag{A.2.3}$$

$$\left\{\frac{d}{d\xi}\left[\left(\xi^2 \mp 1\right)\frac{d}{d\xi}\right] - \left[\lambda_{mn} - c^2\xi^2 - \frac{m^2}{\xi^2 \mp 1}\right]\right\}\begin{matrix} R_{mn}(c,\xi) \\ R_{mn}(-ic,i\xi) \end{matrix} = 0 \tag{A.2.4}$$

Note that for $c = 0$, (A.2.3) reduces to the scalar spherical harmonic differential equation.

All these differential equations submit to the form

$$\frac{d}{dz}\left[\left(1-z^2\right)\frac{du}{dz}\right] + \left[\lambda - c^2z^2 - \frac{\mu^2}{1-z^2}\right]u = 0 \tag{A.2.5}$$

Any solution of the above equation for arbitrary values of the separation constants λ and μ with $c^2 \neq 0$ is, in general, called a spheroidal function.

A.3 Power series expansion for λ_{mn}

For small values of the c parameter, the λ eigenvalue admits to a power series expansion. Note that, as expected, only even powers of c show up.

$$\lambda_{mn} = \sum_{k=0}^{\infty} l_{2k} c^{2k} \tag{A.3.1}$$

The formulas for the l_k's become increasingly cumbersome for higher order terms so, here, we only quote the first three non-zero ones.

$$l_0 = n(n+1) \tag{A.3.2a}$$

$$l_2 = \frac{1}{2}\left[1 - \frac{(2m-1)(2m+1)}{(2n-1)(2n+3)}\right] \tag{A.3.2b}$$

$$\begin{aligned} l_4 = & \frac{(n-m-1)(n-m)(n+m-1)(n+m)}{2(2n-3)(2n-1)^3(2n+1)} \\ & - \frac{(n-m+1)(n-m+2)(n+m+1)(n+m+2)}{2(2n+1)(2n+3)^3(2n+5)} \end{aligned} \tag{A.3.2c}$$

Details on the computation of this expansion as well as more terms an be found in [28; 29].

A.4 Asymptotic expansions of λ_{mn}

In this section, we are interested in the asymptotic expansion of λ_{mn} for large values of the parameter c. Care must be taken for one to differentiate between the oblate and prolate case or equivalently whether c is real or imaginary.

Details on the computation of this expansion can be found in [28; 29] along with tabulated values. Here, we quote the results used in this thesis. They hold for $c \to \infty$. For the prolate eigenvalues

$$\lambda_{mn}(c) = pc + \left(m^2 - \frac{p^2+5}{8}\right) + O\left(\frac{1}{c}\right) \quad \text{where} \quad p = 2(n-m)+1 \tag{A.4.1}$$

while for the oblate

$$\begin{aligned} \lambda_{mn}(-ic) = & -c^2 + 2\left(2\nu + m + 1\right)c \\ & - \left[2\nu\left(\nu + m + 1\right) + (m+1)\right] + O\left(\frac{1}{c}\right) \end{aligned} \tag{A.4.2}$$

where ν is promptly defined by $\nu = \begin{cases} \frac{n-m}{2}\,, & (n-m) \text{ even} \\ \frac{n-m-1}{2}\,, & (n-m) \text{ odd} \end{cases}$. Note that for $\lambda_{ml}(z)$, the decrease of $\arg z$ from 0 to $-\pi/2$ introduces a $\sim z^2$ dependence in the asymptotic expansion $|z| \to \infty$.

APPENDIX B

The Hypergeometric Function

The hypergeometric function ${}_2F_1$ is important both for mathematics and physics. Many physical and mathematical problems have solutions in terms of it and as such it has very rich mathematical properties. The purpose of this appendix is not to provide a comprehensive review but to present the reader with a brief introduction.

B.1 The hypergeometric differential equation

The hypergeometric differential equation is a second-order linear ordinary differential equation with three regular singular points. at $x = 0, 1, \infty$ [30] .

$$u''(z) + \frac{(\alpha+\beta+1)z-\gamma}{z(z-1)}u'(z) + \frac{\alpha\beta}{z(z-1)}u(z) = 0 \tag{B.1.1}$$

The generalized version of this equation to three arbitrary singular points in the complex plane is given by *Riemann's differential equation*. Every second-order ODE with three regular singular points can be transformed into the hypergeometric by a change of variables.

B.2 The solution

The solution to the hypergeometric differential equation is given by the hypergeometric series

$$\begin{aligned} {}_2F_1(\alpha,\beta,\gamma;\ z) &= \sum_{n=0}^{\infty} \frac{(\alpha)_n(\beta)_n}{(\gamma)_n}\frac{z^n}{n!}\ , \quad |z|<1 \\ &= \frac{\Gamma(\gamma)}{\Gamma(\alpha)\Gamma(\beta)}\sum_{n=0}^{\infty}\frac{\Gamma(\alpha+n)\Gamma(\beta+n)}{\Gamma(\gamma+n)}\frac{z^n}{n!}\ , \quad |z|<1 \end{aligned} \tag{B.2.1}$$

where $(x)_n$ is the Pochhammer symbol defined by

$$(x)_n = \begin{cases} 1 & \text{if} \quad n=0 \\ x(x+1)\dots(x+n-1) & \text{if} \quad n>0 \end{cases} \tag{B.2.2}$$

The series (B.2.1) is defined and convergent when [29]

- $-\gamma \notin \mathbf{N}$, i.e. γ is not a negative integer.
- $\Re\{\gamma - \alpha - \beta\} > -1$

The two linearly independent solutions around the regular singular point $z = 0$ are

$$f_1^0(z) = {}_2F_1(\alpha, \beta, \gamma;\ z) \tag{B.2.3a}$$
$$f_2^0(z) = z^{1-\gamma}{}_2F_1(1+\alpha-\gamma, 1+\beta-\gamma, 2-\gamma;\ z) \tag{B.2.3b}$$

The solution can be analytically extended to the whole complex plane and by using various transformation properties (see [29]) the solutions can be expressed around $z = 1$

$$f_1^1(z) = {}_2F_1(\alpha, \beta, 1+\alpha+\beta-\gamma;\ 1-z) \tag{B.2.4a}$$
$$f_2^1(z) = (1-z)^{\gamma-\alpha-\beta}{}_2F_1(\gamma-\beta, \gamma-\alpha, 1-\alpha-\beta+\gamma;\ 1-z) \tag{B.2.4b}$$

and around $z = \infty$ as

$$f_1^\infty(z) = z^{-\alpha}{}_2F_1(\alpha, 1+\alpha-\gamma, 1+\alpha-\beta;\ z^{-1}) \tag{B.2.5a}$$
$$f_2^\infty(z) = z^{-\beta}{}_2F_1(\beta, 1+\beta-\gamma, 1+\beta-\alpha;\ z^{-1}) \tag{B.2.5b}$$

Of course, these can be written as linear combinations of one another. For example,

$$f_1^0(z) = \frac{\Gamma(\gamma)\Gamma(\gamma-\alpha-\beta)}{\Gamma(\gamma-\alpha)\Gamma(\gamma-\beta)} f_1^1(z) + \frac{\Gamma(\gamma)\Gamma(\alpha+\beta-\gamma)}{\Gamma(\alpha)\Gamma(\beta)} f_2^1(z) \tag{B.2.6a}$$
$$= \frac{\Gamma(\gamma)\Gamma(\beta-\alpha)}{\Gamma(\beta)\Gamma(\gamma-\alpha)} f_1^\infty(z) + \frac{\Gamma(\gamma)\Gamma(\alpha-\beta)}{\Gamma(\alpha)\Gamma(\gamma-\beta)} f_2^\infty(z) \tag{B.2.6b}$$

APPENDIX C

Mathematica Source Code

C.1 Monodromy source code

The following Mathematica code was used for computing the quasi-normal modes in §5.3 according to the Monodromy method presented in §4.3

The **ffuncs**[] module computes the f_i's of (4.3.35). They are dependent only on the angular momentum $a = MJ$ of the black hole. Knowing these is enough to compute all highly damped QNMs for every angular parameter set (l, m) and black hole mass M. [1]

```
ffuncs[J_] := Module[
  { δ̃2, δ̃1, δ̃0,
    Q̃2, Q̃1,
    int2, int1, int0,
    t2, t1, Δ, r+, r−, x,
    M=1, r = M x, a = M J
  },
```

Definitions of Δ, the horizons $r_\pm$, $\tilde{Q}_i$'s (given in (4.3.3) except from a factor of m in $\tilde{Q}_1$) and the two conjugate roots of $\tilde{Q}_2$, t_1 and $t_2 = t_1^*$.

```
  Δ[x_] = r^2 − 2Mr + a^2;
  {r−, r+} = x /. Solve[Δ[x] == 0, x] // Sort;

  {Q̃2[x_], Q̃1[x_]}=
    {
      (r^2 + a^2)^2 − a^2 Δ[x],
      −4Mra
    } //Simplify;
  {t1, t2} = ( x /. Solve[ Q̃2[x]==0, x] // Simplify) [[3;;4]] //Sort;
```

[1] Setting $M = 1$ essentially rescales as per (5.1.1).

Calculation of $\tilde{\delta}_i$'s: The integration has to be over a contour which belongs in the same equivalence class as l_2 (see Fig.4.1). **NIntegrate**[] integrates over a straightline connecting the two points of integration which, when $r_- < \Re t_i < r_+$, is sufficient. However, in case $\Re t_i > r_+$ or $\Re t_i < r_-$ (which happens for some values of J), this default integration contour will be non-equivalent to l_2. We thus remedy this once and for all by giving $\frac{r_+ - r_-}{2}$ as an intermediate integration point thereby forcing the contour to be equivalent to l_2 for all values of J.

```
17   int2[x_] = Sqrt[Q̃2[x]] / Δ[x] // Simplify;
18   int1[x_] = Q̃1[x] / (2Sqrt[Q̃2[x]]Δ[x]) // Simplify;
19   int0[x_] = M^2 / (2Sqrt[Q̃2[x]]);
20
21   δ̃2 = 2π(r+^2 + a^2) − iM(r+ − r−) NIntegrate[ int2[x], {x, t1, (r+ + r−)/2, t2}];
22   δ̃1 = 2πa + i(r+ − r−) NIntegrate[ int1[x], {x, t1, (r+ + r−)/2, t2}];
23   δ̃0 = −2ia(r+ − r−) NIntegrate[ int0[x], {x, t1 ,(r+ + r−)/2, t2}]/M;
```

Return value of the module is the list $\{f_0, f_1, f_2, f_3\}$:

```
24   {
25     δ̃1/δ̃2 ,
26     (δ̃0 + π(r+ − r−))/(2δ̃2) ,
27     π(r+ − r−)/δ̃2 ,
28     δ̃0/δ̃2
29   }
30 ];
```

Bibliography

[1] E. Berti1, V. Cardoso1, and A. O. Starinets, "Quasinormal modes of black holes and black branes," *arXiv:0905.2975v2 [gr-qc]*, 2009.

[2] V. Cardoso, "Quasinormal modes and gravitational radiation in black hole spacetimes," 2003. Ph.D. Thesis (Advisor: Jose Pizarro de Sande e Lemos).

[3] J. M. Weisberg and J. H. Taylor, "Relativistic binary pulsar B1913+16: Thirty years of observations and analysis," *ASP Conf.Ser.*, vol. 328, p. 25, 2005.

[4] M. Pitkin, S. Reid, S. Rowan, and J. Hough, "Gravitational Wave Detection by Interferometry (Ground and Space)," 2011.

[5] J. D. Bekenstein, "Black holes: Classical properties, thermodynamics, and heuristic quantization," 1998.

[6] S. Bhattacharya and A. Lahiri, "No hair theorems for stationary axisymmetric black holes," 2011.

[7] S. Hawking, "Black hole explosions?," *Nature*, vol. 248, pp. 30–31, Mar. 1974.

[8] J. Preskill, "Do black holes destroy information?," 1992.

[9] S. W. Hawking, "Information Loss in Black Holes," *Phys. Rev.*, vol. D72, p. 084013, 2005.

[10] J. M. Maldacena, "Eternal black holes in Anti-de-Sitter," *JHEP*, vol. 04, p. 021, 2003.

[11] A. G. Riess *et al.*, "Observational Evidence from Supernovae for an Accelerating Universe and a Cosmological Constant," *Astron. J.*, vol. 116, pp. 1009–1038, 1998.

[12] S. Perlmutter *et al.*, "Measurements of Omega and Lambda from 42 High-Redshift Supernovae," *Astrophys. J.*, vol. 517, pp. 565–586, 1999.

[13] N. Voje Johansen and F. Ravndal, "On the discovery of Birkhoff's theorem," *ArXiv Physics e-prints*, Aug. 2005.

[14] S. M. Carroll, *An introduction to Spacetime and Geometry.* Addison Wesley, 2004.

[15] P. K. Townsend, "Black holes," *arXiv: gr-qc/9707012*, 1997.

[16] R. H. Boyer and R. W. Lindquist, "Maximal Analytic Extension of the Kerr Metric," *Journal of Mathematical Physics*, vol. 8, pp. 265–281, Feb. 1967.

[17] D. Raine and E. Thomas, *Black Holes: An Introduction*. Imperial College Press, 2005.

[18] S.Chandrasekhar, *The Mathematical Theory of Black Holes*. Oxford University Press, 1983.

[19] D. R. Brill, P. L. Chrzanowski, and C. M. Pereira, "Solution of the scalar wave equation in a kerr background by separation of variables," *Phys. Rev. D.*, vol. 5, Apr 1972.

[20] S. A. Teukolsky, "Rotating black holes: Separable wave equations for gravitational and electromagnetic perturbations," *Phys. Rev. Lett.*, vol. 29, pp. 1114–1118, Oct 1972.

[21] M. Banados, C. Teitelboim, and J. Zanelli, "The Black hole in three-dimensional spacetime," *Phys. Rev. Lett.*, vol. 69, pp. 1849–1851, 1992.

[22] V. Cardoso and J. P. Lemos, "Scalar, electromagnetic and Weyl perturbations of BTZ black holes: Quasinormal modes," *Phys.Rev.*, vol. D63, p. 124015, 2001. Latex, 14 pages.

[23] N. Fröman and P. O. Fröman, *JWKB Approximation: Contributions to the Theory*. North-Holland Publishing Company, Amsterdam, 1965.

[24] A. B. O. Daalhuis, S. J. Chapman, J. R. King, J. R. Ockendon, and R. H. Tew, "Stokes phenomenon and matched asymptotic expansions," *SIAM Journal on Applied Mathematics*, vol. 55, no. 6, pp. 1469–1483, 1995.

[25] D. V. Gal'tsov and A. A. Matiukhin, "Matrix wkb method for black hole normal modes and quasibound states," *Classical and Quantum Gravity*, vol. 9, no. 9, p. 2039, 1992.

[26] U. Keshet and S. Hod, "Analytic Study of Rotating Black-Hole Quasinormal Modes," *Phys. Rev.*, vol. D76, p. 061501, 2007.

[27] H.-c. Kao and D. Tomino, "Quasinormal Modes of Kerr Black Holes in Four and Higher Dimensions," *Phys.Rev.*, vol. D77, p. 127503, 2008.

[28] C. Flammer, *Spheroidal Wave Functions*. Stanford University Press, 1957.

[29] M. Abramowitz and I. A. Stegun, *Handbook of Mathematical Functions*. Dover Publications, Inc., New York, 1965.

[30] G. Kristensson, *Second Order Differential Equations: Special Functions and Their Classification*. Springer, 2010.